

ASTRO
SCIENCES
CENTER



N 67 12224

FACILITY FORM 802

(ACCESSION NUMBER)	(THRU)
62	1
(PAGES)	(CODE)
CR 79297	30
(NASA CR OR TMX OR AD NUMBER)	(CATEGORY)

GPO PRICE \$ _____

CFSTI PRICE(S) \$ _____

Hard copy (HC) 3.00

Microfiche (MF) 75

ff 853 July 85

Report No. T-17

LOW-THRUST TRAJECTORY CAPABILITIES
FOR EXPLORATION OF THE SOLAR SYSTEM
USING NUCLEAR ELECTRIC PROPULSION



Report No. T-17

LOW-THRUST TRAJECTORY CAPABILITIES
FOR EXPLORATION OF THE SOLAR SYSTEM
USING NUCLEAR ELECTRIC PROPULSION

by

A. L. Friedlander

Astro Sciences Center

of

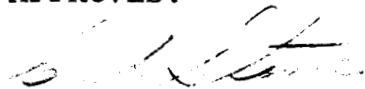
IIT Research Institute
Chicago, Illinois

for

Lunar and Planetary Programs
Office of Space Science and Applications
NASA Headquarters
Washington, D. C.

Contract No. NASr-65(06)

APPROVED:



C. A. Stone, Director
Astro Sciences Center

October 1966

IIT RESEARCH INSTITUTE

SUMMARY

This report presents the trajectory energy requirements for low-thrust (electric propulsion) flight throughout the solar system, first for the general class of flyby missions to points in and above the ecliptic plane, and then for flyby, capture and orbiter missions to the planets Mercury through Pluto. The trajectory energy requirements are described in terms of the parameter "J" - defined as the time integral of thrust acceleration squared. Application of these results is for the most part limited to electric propulsion systems operating at constant power, i.e., nuclear-electric systems. Neither solar electric nor hybrid low thrust systems have been considered. Nevertheless the results of this study are important for reference and comparison in the advanced planning of solar system exploration.

Results for the general class of flyby missions are presented as accessible regions contours of J and flight time. The accessible regions concept provides a convenient graphical means of characterizing and comparing the performance capability of different vehicle systems and modes of propulsion. Results for the planetary missions are presented as graphs of J vs flight time.

The payload/flight time capabilities of two conceptual nuclear-electric spacecraft designs are illustrated in terms of the accessible regions graph and summarized for each of the

planetary missions. The two powerplant specific weights assumed here are 41.6 and 25 lb/kwj, corresponding to thruster power levels of 240 and 400 kwj, respectively. These numbers obviously represent a rather advanced powerplant technology.

Assuming that this technology will become a reality in the not too distant future, it is shown that the application of nuclear-electric propulsion systems to upper stage space vehicles offers a high performance potential for carrying out a long-range plan of solar system exploration. This performance potential (large payloads and reduced flight time) is particularly in evidence when the mission energy requirements are very high. On the basis of results described in this report and previous comparisons between ballistic and thrusting flight, the most attractive applications of nuclear-electric propulsion for unmanned exploration are identified with solar probes, out-of-the-ecliptic probes, Neptune and Pluto flybys, minimal capture orbiters at Uranus and beyond, and low altitude circular orbiters about all the outer planets.

TABLE OF CONTENTS

	<u>Page</u>
1. INTRODUCTION	1
2. PARAMETERS OF ELECTRIC PROPULSION SYSTEMS	3
3. ACCESSIBLE REGIONS CONTOURS	5
4. J REQUIREMENTS FOR PLANETARY FLIGHT	18
5. EXAMPLES OF PAYLOAD CAPABILITY	43
6. CONCLUSIONS	51
Appendix A - NOMENCLATURE	53
REFERENCES	54

LIST OF FIGURES

	<u>Page</u>
1. The Plane P_N , Showing Basic Geometry of the Accessible Regions Method	9
2. J Contours for 100 Day Fly-by Trajectories	10
3. J Contours for 300 Day Fly-by Trajectories	11
4. J Contours for 500 Day Fly-by Trajectories	12
5. J Contours for 750 Day Fly-by Trajectories	13
6. J Contours for 1000 Day Fly-by Trajectories	14
7. Time of Flight Contours for Heliocentric Fly-by Trajectories with J Capability of $10 \text{ m}^2/\text{sec}^3$	15
8. Time of Flight Contours for Heliocentric Fly-by Trajectories with J of $20 \text{ m}^2/\text{sec}^3$	16
9. Accessible Regions Comparison of Variable and Constant Thrust Modes for 500 Day Flights and J Capability of $20 \text{ m}^2/\text{sec}^3$	17
10. Earth-Escape Requirements	25
11. Planet-Capture Requirements for Circular Orbit at Three Planet Radii	26
12. J Requirements for Fly-by Missions to the Inner Planets	27
13. J Requirements for Parabolic Capture Missions to the Inner Planets	28
14. J Requirements for Orbiter Missions to the Inner Planets	29

LIST OF FIGURES (Cont'd)

	<u>Page</u>
15. J Requirements for Fly-by Missions to the Outer Planets	30
16. J Requirements for Parabolic Capture Missions to the Outer Planets	31
17. J Requirements for Orbiter Missions to the Outer Planets	32
18. J Requirements for Missions to Mercury	33
19. J Requirements for Missions to Venus	34
20. J Requirements for Missions to Mars	35
21. J Requirements for Missions to Jupiter	36
22. J Requirements for Missions to Saturn	37
23. J Requirements for Missions to Uranus	38
24. J Requirements for Missions to Neptune	39
25. J Requirements for Missions to Pluto	40
26. Performance Curves for Two Conceptual Designs of Nuclear-Electric Spacecraft	46
27. Accessible Regions Comparison of Low-Thrust and Ballistic Launch Vehicles Each Delivering a 500 lb Communications and Experiments Payload	47
28. Accessible Regions Comparison of Low Thrust and Ballistic Launch Vehicles Each Delivering a 2000 lb Communications and Experiments Payload	48

LIST OF TABLES

	<u>Page</u>
1. Phase Breakdown of a Typical Orbiter Mission to Mercury	41
2. Range of Approach Hyperbolic Velocities for Minimum J Flyby Missions	42
3. Flight Times for Low-Thrust Missions to the Inner Planets	49
4. Flight Times for Low-Thrust Missions to the Outer Planets	50

LOW-THRUST TRAJECTORY CAPABILITIES
FOR EXPLORATION OF THE SOLAR SYSTEM
USING NUCLEAR ELECTRIC PROPULSION

1. INTRODUCTION

This summary of trajectory requirements is intended to provide supporting data in a convenient form to aid in evaluating the performance potential of electric propulsion for carrying out future exploration of the solar system. The results presented herein are essentially limited to (1) thruster operation at constant power, i.e., nuclear-electric powerplants, and (2) all-electric propulsion including planetocentric maneuvers, i.e., hybrid propulsion systems are not considered. It is realized, of course, that each of these assumptions is at present subject to considerable argument based on the projected state-of-the-art and, therefore, may not represent the best application of electric propulsion over the next several decades. Nevertheless, the results themselves should be useful for reference and comparison purposes.

Trajectory energy requirements are first described for the general class of flyby missions throughout the solar system,

both in and above the ecliptic plane. These results are presented as accessible regions performance contours; a form of data presentation particularly suited to mission survey purposes (Narin 1964). The accessible regions concept provides a convenient graphical means of characterizing and comparing the performance capability of different vehicle systems and modes of propulsion (Friedlander 1965, Friedlander and Narin 1966). Trajectory requirements are then presented for specific planetary missions. Flyby, capture and orbiter missions to each of the planets Mercury through Pluto are considered.

The basic data used in this report were obtained from numerical integration solutions of optimal heliocentric trajectories assuming a variable thrust mode of operation. Supplementary data were taken from an earlier JPL report (Melbourne 1961). Trajectory energy requirements are also given for constant thrust flight which is considered to be the more practical mode of thruster operation. The constant thrust results are obtained from the "exact" variable thrust data by an approximation method known as "characteristic length correlation" (Zola 1964). The accuracy of this approximation has been estimated to be within a few percent (Friedlander 1965).

2. PARAMETERS OF ELECTRIC PROPULSION SYSTEMS

In any analysis which attempts to relate trajectory requirements and vehicle performance it is necessary to have a suitable "link" between the trajectory kinematics and the vehicle/propulsion system characteristics. For ballistic flights, the trajectory energy requirements are expressed in terms of ideal velocity (ΔV) which is readily related to launch vehicle payload capability. The somewhat analogous parameter used for low-thrust flight is defined as

$$J = \int_0^{T_f} a^2(t) dt \quad (1)$$

where T_f is the mission flight time and a is the thrust acceleration associated with the mission trajectory. Along with the above definition, the following expressions summarize the link between vehicle, propulsion and trajectory (in the MKS system of units)

$$\begin{aligned} 2P_j &= \dot{M} (g_o I_{SP})^2 \\ &= M a (g_o I_{SP}) \end{aligned} \quad (2)$$

$$\frac{M_{PL}}{M_o} = \frac{M_{PP}}{M_o} \left[\frac{1}{\frac{M_{PP}}{M_o} + \frac{J\alpha_j}{2}} - 1 \right] \quad (3)$$

$$\alpha_j = \frac{M_{PP}}{P_j} \quad (4)$$

where P_j is the kinetic power developed in the exhaust jet, \dot{M} is the propellant flow rate, I_{SP} is the specific impulse, and

g_0 is 9.806 m/sec^2 . The initial vehicle mass (M_0) is allocated into powerplant (M_{PP}), net payload (M_{PL}) and propellant ($M_0 - M_{PP} - M_{PL}$). For nuclear-electric powerplants, M_{PP} would consist of the entire propulsion system, i.e., reactor, shield, radiators, power conversion and conditioning, and thrusters. Net payload might typically be broken down into structure, tankage, guidance and control, and scientific experiments including communication and data handling equipment.

Equation (3) shows that the most important factors affecting payload capability are J and the specific mass of the powerplant, α_j . Clearly, low values for both parameters are desirable. J is minimized by the choice of an optimum trajectory for each mission. This includes an optimum launch date and thrust direction program, and, in the case of constant thrust operation, an optimum specific impulse and propulsion-on time.

The nuclear-electric powerplant size most desirable for unmanned interplanetary exploration is of the 200-500 kw class (Fimple 1965, Brown 1966). Projected estimates of the specific mass of such powerplants are in the range 25-75 lb/kwj (kwj denotes jet power in kilowatts). It should be emphasized that such lightweight powerplants do not yet exist but are representative of advanced reactor and power-conditioning technology (Lubarsky 1966).

It is of interest to note the practical limitation imposed upon J by the powerplant weight. To illustrate this point, suppose that α_j is 25 lb/kwj and that M_{PP}/M_0 is $1/3$. Further, suppose that the criterion for useful payload is $M_{PL}/M_0 \geq 1/10$. Then, from Equation (3), the maximum value of J is found to be $77 \text{ m}^2/\text{sec}^3$. In

general, the limitation on J capability is inversely proportional to α_j .

3. ACCESSIBLE REGIONS CONTOURS

The basic idea behind the accessible regions concept of data presentation is to portray the three-dimensional solar system as a two-dimensional model. With reference to Figure 1, these two dimensions are the radial distance from the Sun (R), and the latitude measured from the ecliptic plane (β). Reduction to two dimensions is accomplished by assuming that a mission can be launched when Earth is in the proper longitudinal position to minimize the value of J required to intercept a given target in a given time of flight. For simplicity, the Earth is assumed to have a circular orbit in the ecliptic plane. Hence, by choosing an optimum launch date, the target longitude may be eliminated from consideration. Information regarding the date of launch is not directly available from this method. However, for the purpose of long-range mission planning, the exact date of launch is not of immediate importance. It is noted, for example, that the opportunity for minimum J flights to the planets occurs once per synodic period.

Figure 1 illustrates the basic geometry of the accessible regions concept and shows a typical J contour. The figure background is the plane normal to the ecliptic plane. This is essentially a side view of the solar system. For reference purposes, the projections of the planetary orbits on this plane are shown. Every potential target position has a corresponding point in this plane as given by its heliocentric distance and latitude. Each J contour, associated with a

particular flight time, represents the maximum boundary of the spatial region accessible to a space vehicle having that J capability. All points within this boundary may be reached either with a lower value of J or a shorter flight time. Since symmetry exists about the ecliptic plane, only the upper halves of the contours are drawn.

Figures 2 through 6 show accessible regions J contours for minimum J flyby flights of 100, 300, 500, 750 and 1000 days, respectively. Regions of the solar system out to 50 AU are covered. In reading these figures it is recalled that the horizontal and vertical scales are, respectively, distances in and normal to the ecliptic plane.

The basic data used in constructing the contours were obtained from numerical integration solutions of optimum trajectories; these solutions being implemented by the JPL Low-Thrust Trajectory Optimization Code (Richardson 1963). J requirements for the Earth-escape phase of a mission are not shown in Figures 2-6, but will be included in later discussion. The J contours shown here are for the variable thrust mode of propulsion which yields the theoretical upper performance bound for power-limited vehicles.

Several types of information are readily obtained from the accessible regions graphs. The minimum value of J required to reach a given point in the solar system in a given flight time may be quickly estimated by interpolation. Conversely, the

maximum spatial region accessible to a vehicle having a given J capability is conveniently displayed.

Consider, for example, the 300 day contours shown in Figure 3. With a J of $20 \text{ m}^2/\text{sec}^3$ all regions in the ecliptic plane from the near vicinity of the Sun out to 4 AU may be explored. For this same value of J, the maximum attainable height above the ecliptic plane is about 1.1 AU, and the maximum latitude is about 41° . Increasing J to $50 \text{ m}^2/\text{sec}^3$ allows an "over-the-Sun" flight at 0.8 AU, and in-plane flights slightly beyond the orbit of Jupiter.

Since the projections of the planetary orbits are included in the figures, one can determine the range of J required to intercept a planet in each synodic period. Fast flights of 100 days require a J capability of $9.5\text{-}30 \text{ m}^2/\text{sec}^3$ to intercept Mars at any point in its orbit, or $15\text{-}30 \text{ m}^2/\text{sec}^3$ to intercept Mercury. Venus can always be reached in 100 days for a J as small as $5 \text{ m}^2/\text{sec}^3$. For a rather long flight of 1000 days, flyby missions to Saturn may be made for $8\text{-}9 \text{ m}^2/\text{sec}^3$. Pluto, however, can never be reached in this flight time unless J is greater than $70 \text{ m}^2/\text{sec}^3$.

Another way of displaying the accessible regions data is to plot time-of-flight contours for a fixed J capability as illustrated in Figures 7 and 8. Figure 8 shows that for a capability of $20 \text{ m}^2/\text{sec}^3$, 100 day flights extend from Mercury to Mars, 500 day flights from above the Sun to a point midway between Jupiter and Saturn, and 1000 day flights from 5 AU

at 90° latitude to 17 AU in the ecliptic (almost to Uranus).

Since the constant thrust mode of propulsion is considered to be more practical from a thruster design standpoint, it is of interest to indicate the performance degradation relative to the variable thrust mode. An accessible regions graph provides a very good illustration of this. Figure 9 compares the regions accessible in 500 days to vehicles having a J capability of $20 \text{ m}^2/\text{sec}^3$ operating in either the variable or constant thrust modes. For this example, the constant thrust vehicle is assumed to have a propulsion/vehicle constraint of $a_0 I_{SP} = 5.4 \text{ m/sec}$ (or, $P_j/M_0 = 26.5 \text{ watts/kg}$). The performance loss is minimized by choosing the optimum specific impulse, which in this case is about 7500 seconds. The maximum distance reachable in 500 days via constant thrust propulsion is decreased by 0.6 AU, or about 8 percent. All latitudes are still available to the constant thrust vehicle. The effect of a non-optimum specific impulse is also shown; the 4000 sec curve indicating a significant performance loss. A comparison between variable and constant thrust is similar for other values of J and flight times. In general, then, a smaller region is accessible to the constant thrust vehicle, or, alternatively, the same region may be explored only if the J capability is increased or the flight time extended.

THE FIGURE BACKGROUND IS THE PLANE P_N NORMAL TO THE ECLIPTIC PLANE, WITH THE PROJECTIONS OF THE INCLUDED PLANETARY ORBITS SHOWN: DRAWN TO SCALE

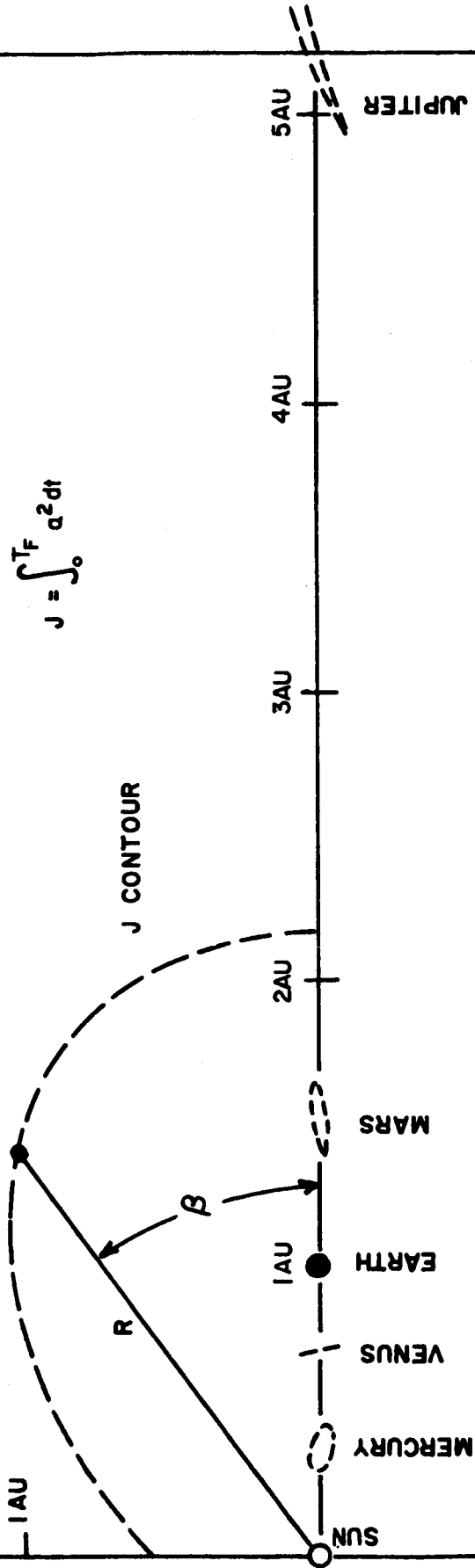


FIGURE 1. THE PLANE P_N , SHOWING BASIC GEOMETRY OF THE ACCESSIBLE REGIONS METHOD, 5AU SCALE.

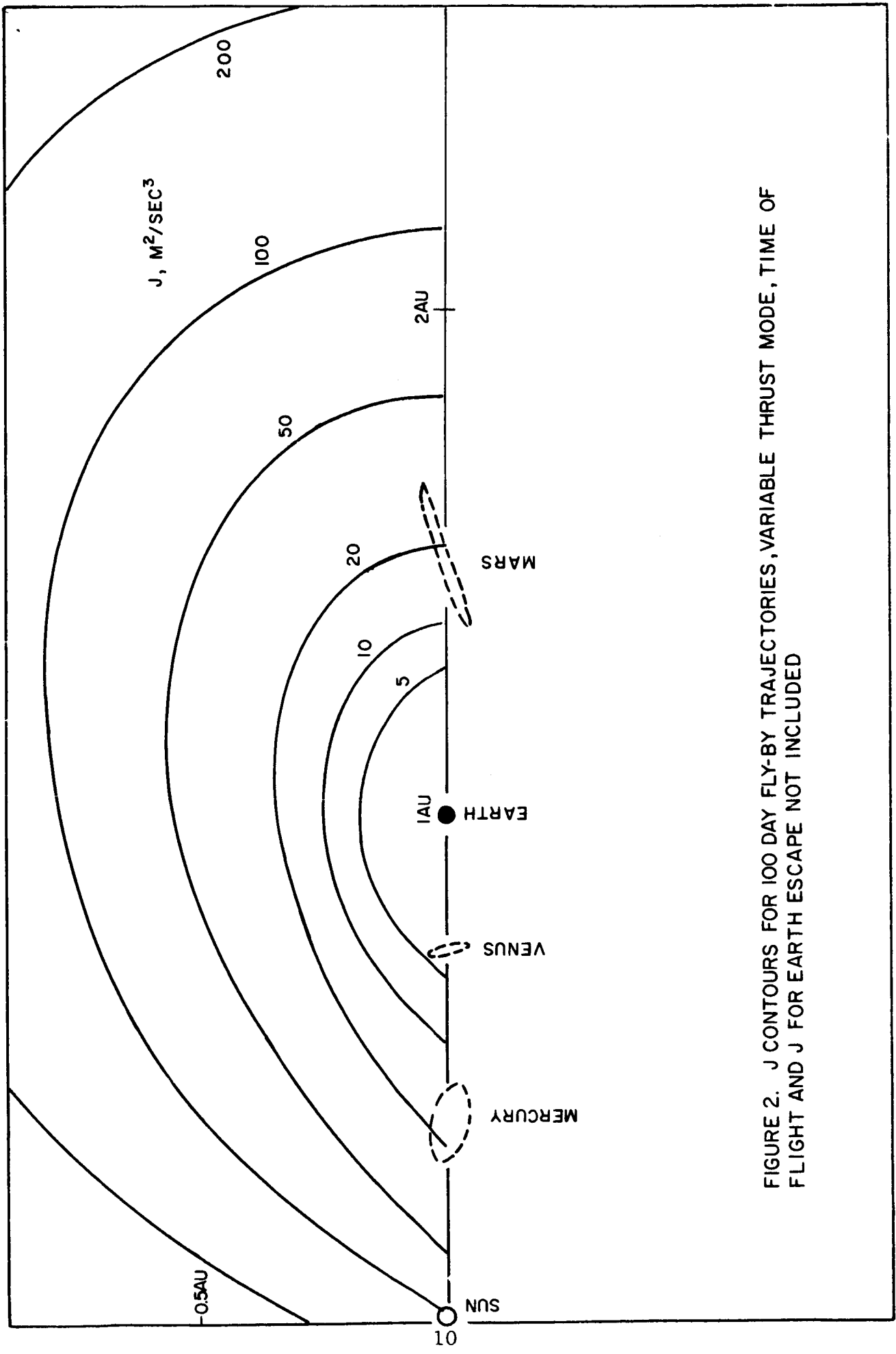


FIGURE 2. J CONTOURS FOR 100 DAY FLY-BY TRAJECTORIES, VARIABLE THRUST MODE, TIME OF FLIGHT AND J FOR EARTH ESCAPE NOT INCLUDED

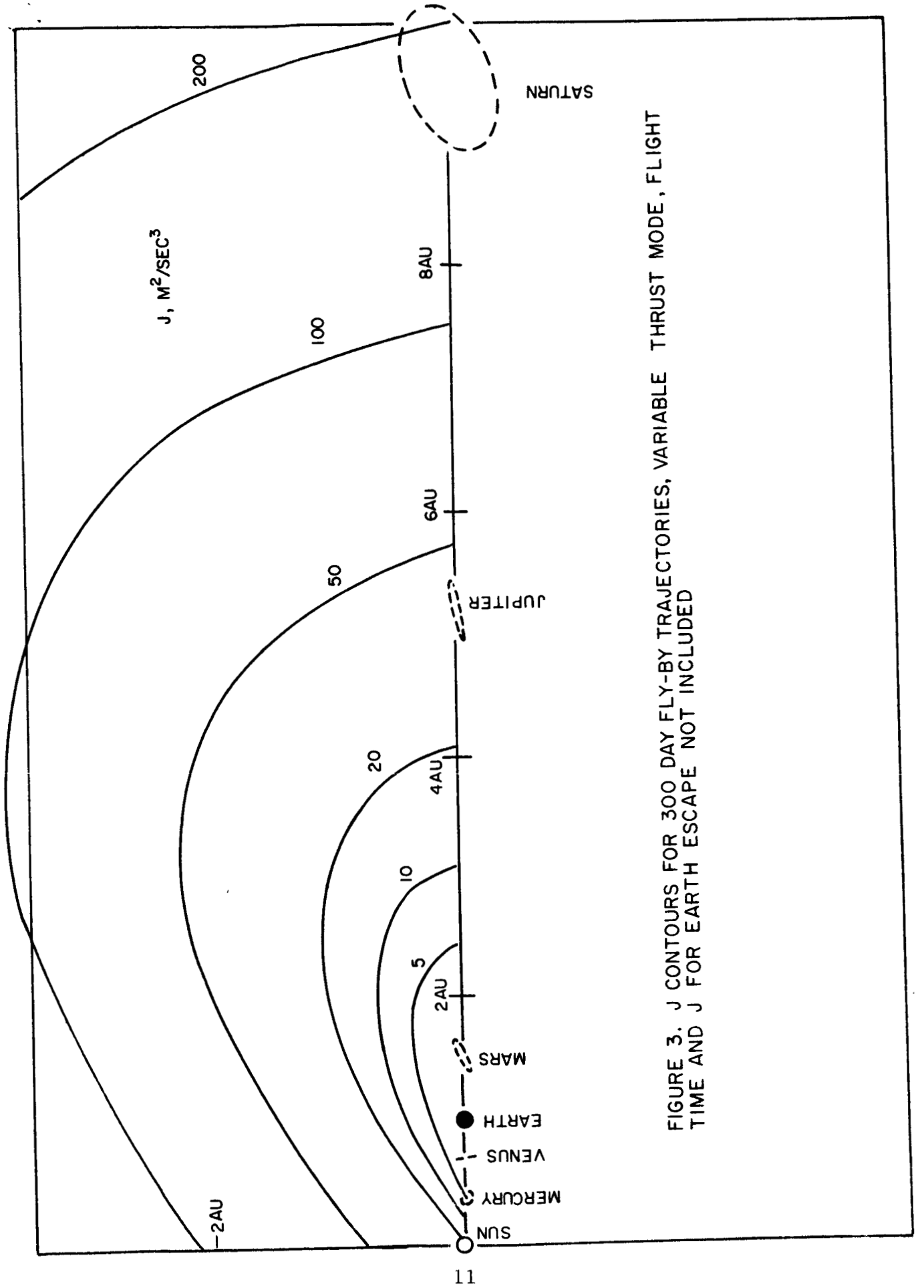


FIGURE 3. J CONTOURS FOR 300 DAY FLY-BY TRAJECTORIES, VARIABLE THRUST MODE, FLIGHT TIME AND J FOR EARTH ESCAPE NOT INCLUDED

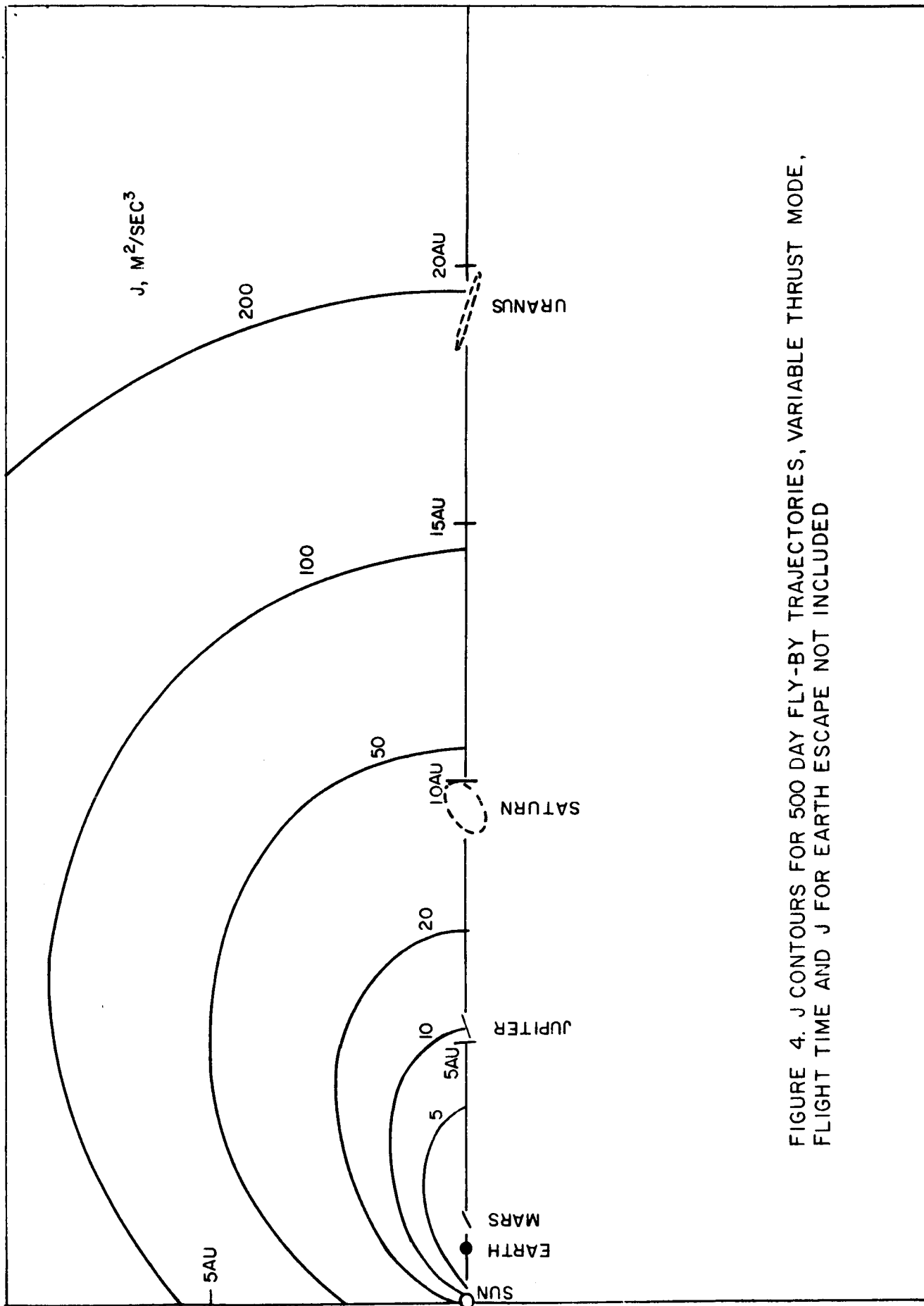


FIGURE 4. J CONTOURS FOR 500 DAY FLY-BY TRAJECTORIES, VARIABLE THRUST MODE, FLIGHT TIME AND J FOR EARTH ESCAPE NOT INCLUDED

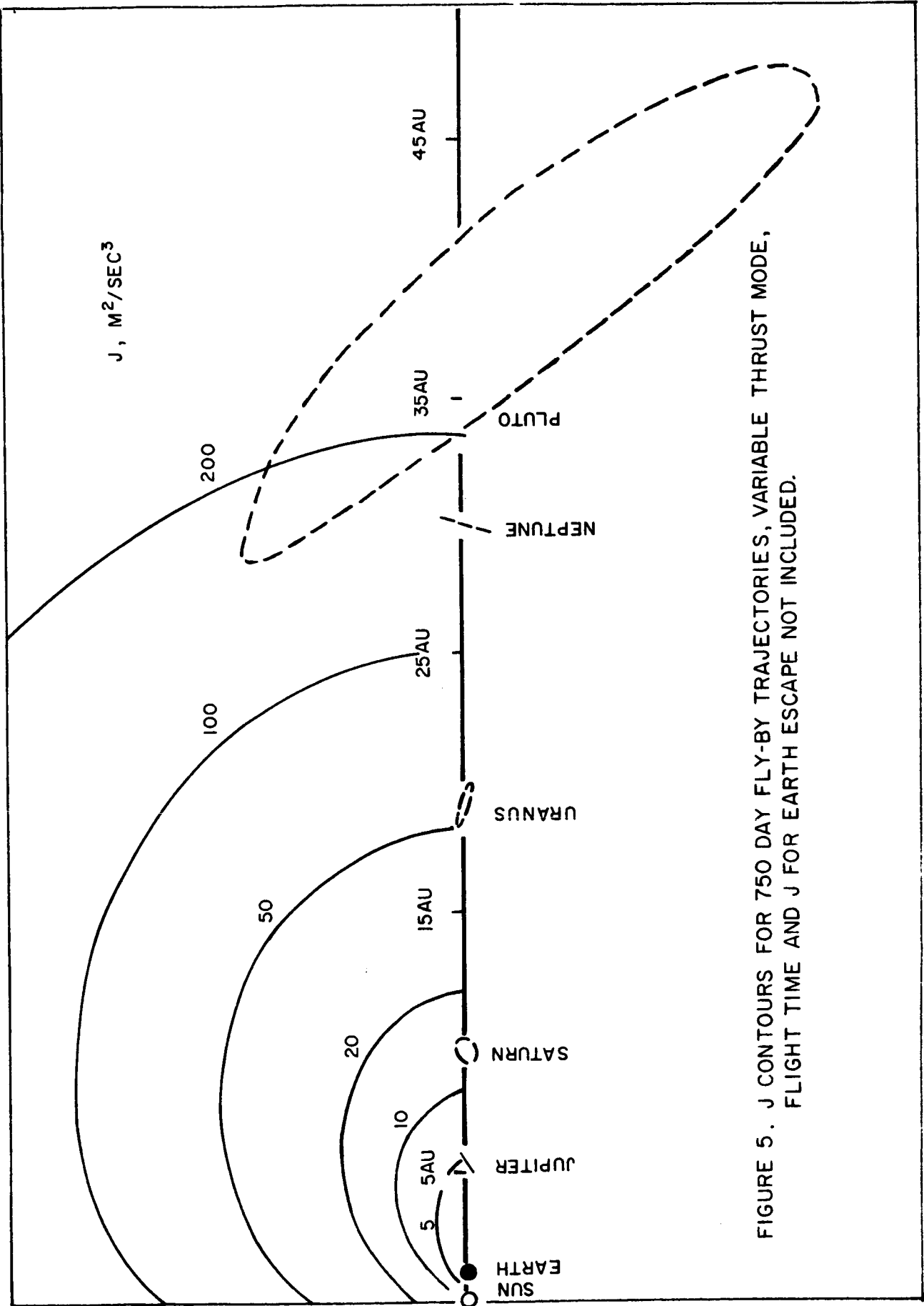


FIGURE 5. J CONTOURS FOR 750 DAY FLY-BY TRAJECTORIES, VARIABLE THRUST MODE, FLIGHT TIME AND J FOR EARTH ESCAPE NOT INCLUDED.

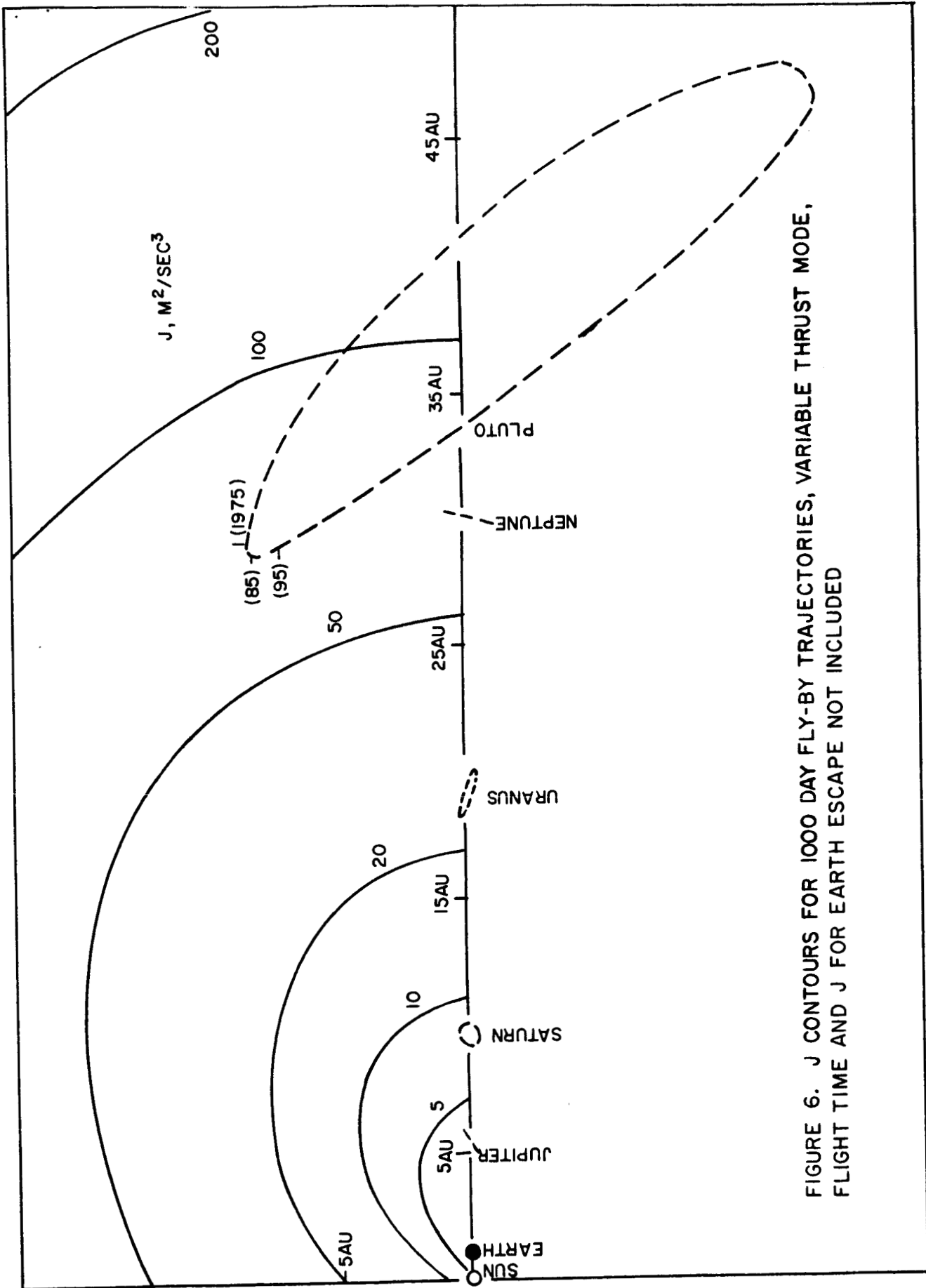


FIGURE 6. J CONTOURS FOR 1000 DAY FLY-BY TRAJECTORIES, VARIABLE THRUST MODE, FLIGHT TIME AND J FOR EARTH ESCAPE NOT INCLUDED

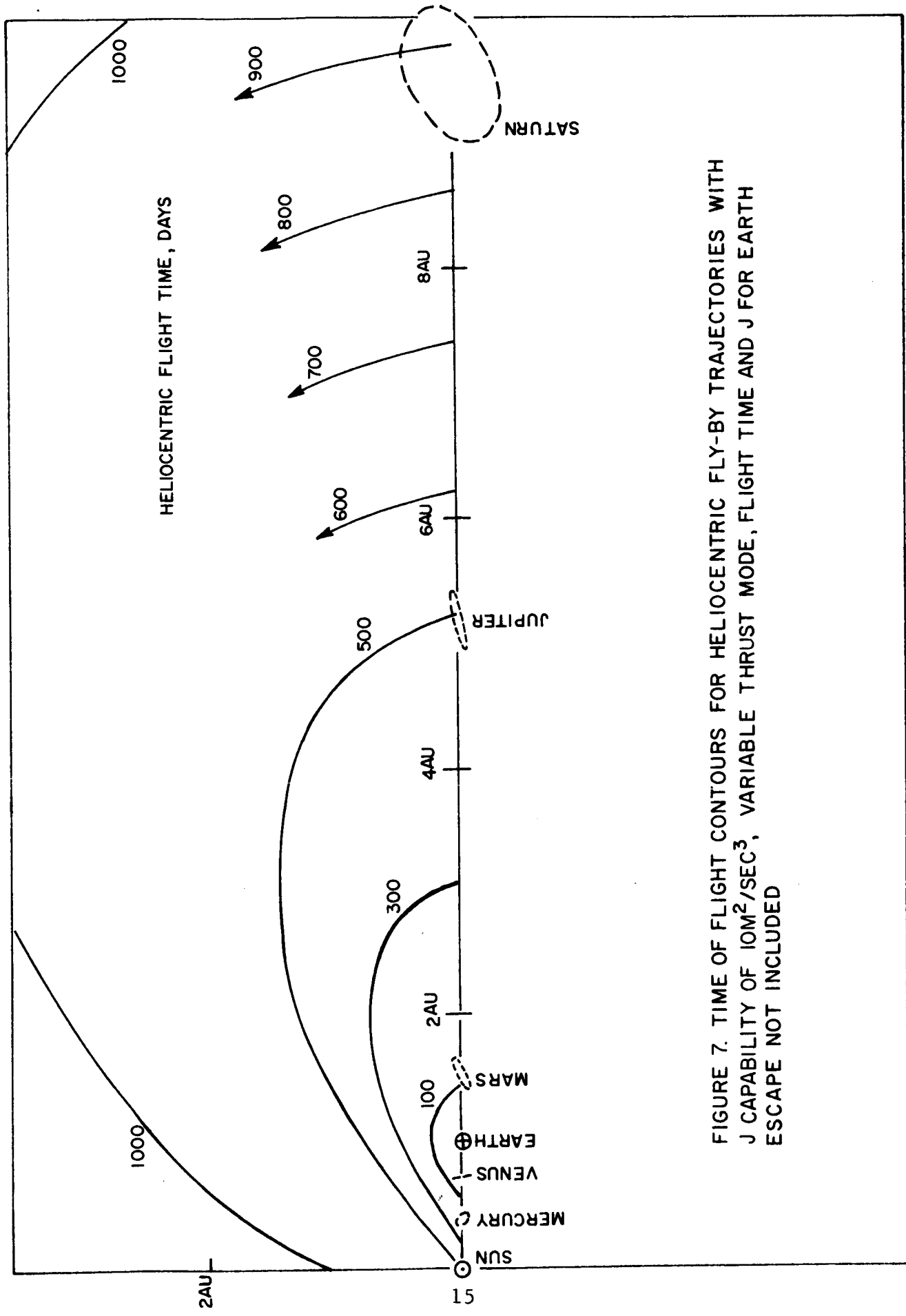


FIGURE 7. TIME OF FLIGHT CONTOURS FOR HELIOCENTRIC FLY-BY TRAJECTORIES WITH
 J CAPABILITY OF $10M^2/SEC^3$, VARIABLE THRUST MODE, FLIGHT TIME AND J FOR EARTH
 ESCAPE NOT INCLUDED

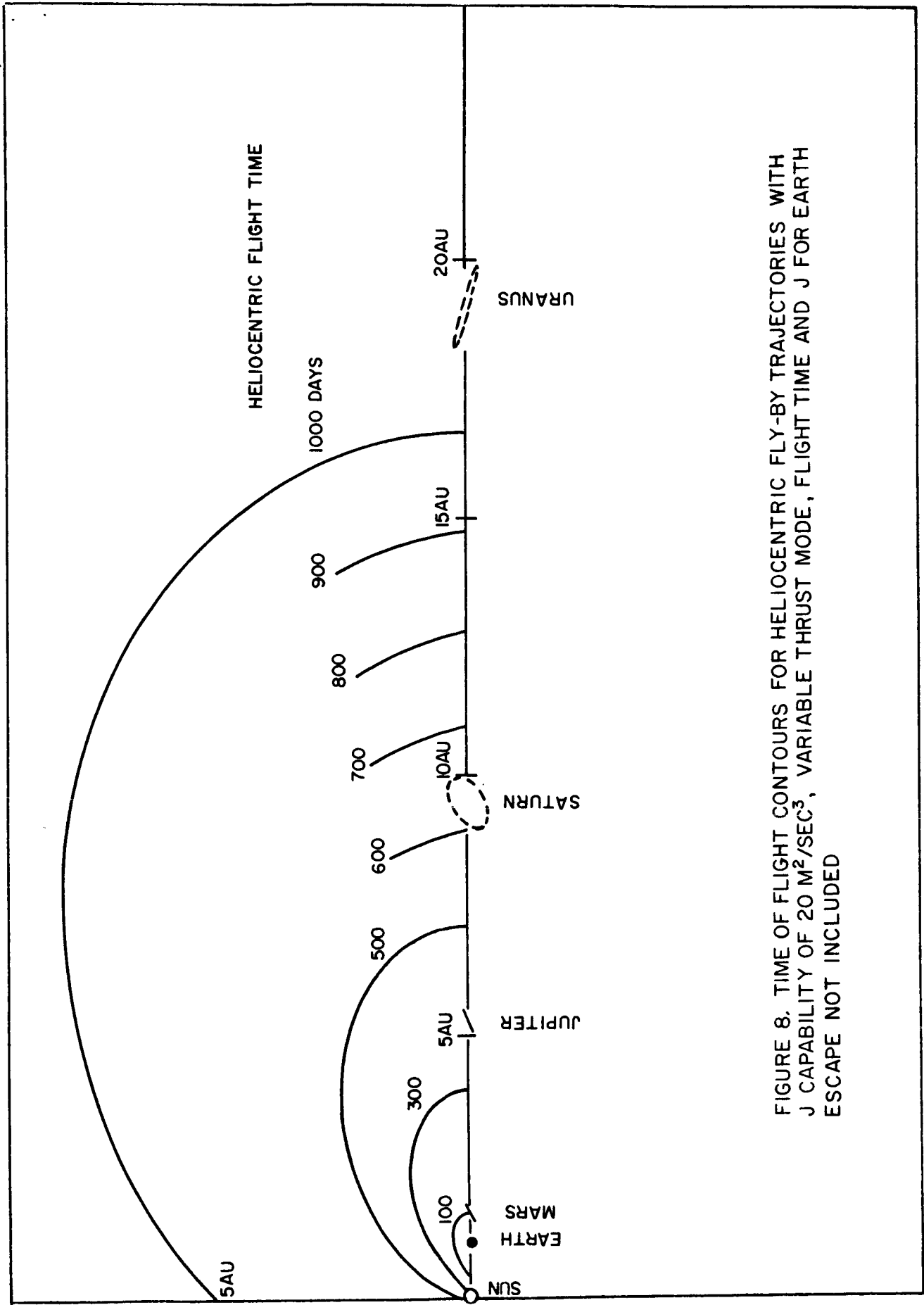


FIGURE 8. TIME OF FLIGHT CONTOURS FOR HELIOCENTRIC FLY-BY TRAJECTORIES WITH J CAPABILITY OF $20 \text{ M}^2/\text{SEC}^3$, VARIABLE THRUST MODE, FLIGHT TIME AND J FOR EARTH ESCAPE NOT INCLUDED

1. VARIABLE THRUST MODE.

CONSTANT THRUST MODE, $a_0|_{sp} = 5.4 \text{ M/SEC}$

- 2. $I_{sp} = 7500 \text{ SEC, OPTIMUM}$
- 3. $9300 \text{ SEC, ALL PROPULSION}$
- 4. 4000 SEC

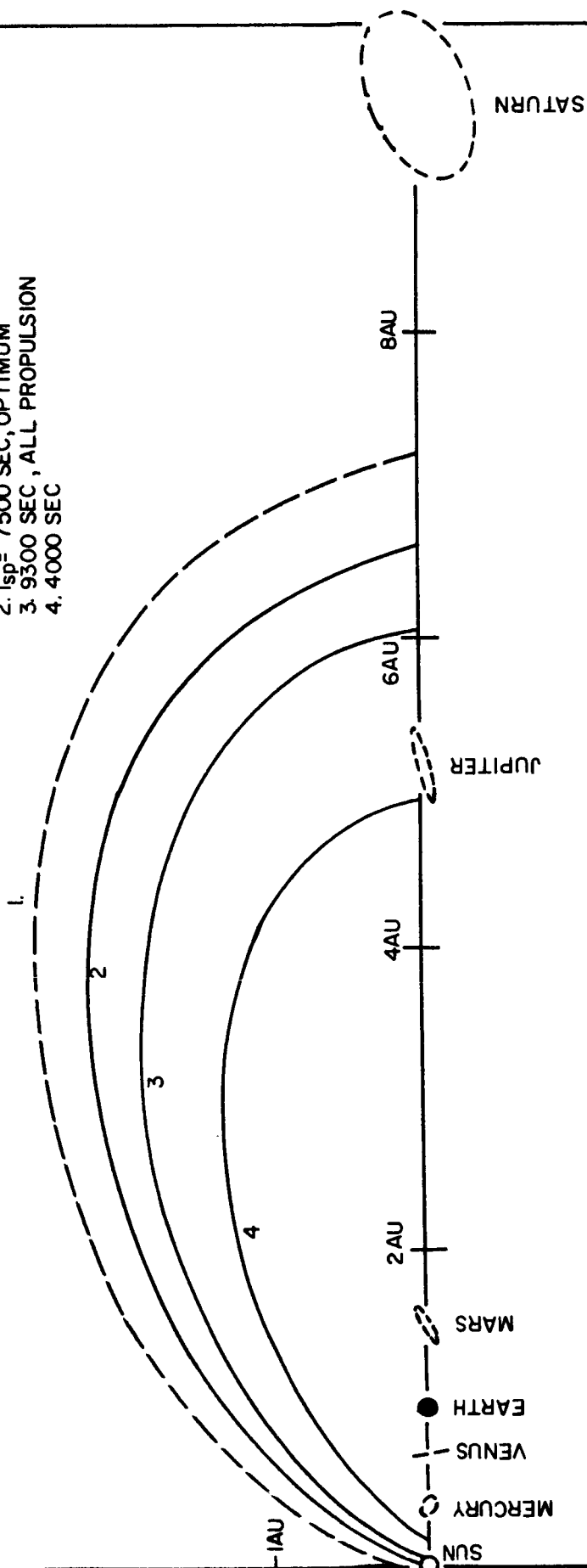


FIGURE 9. ACCESSIBLE REGIONS COMPARISON OF VARIABLE AND CONSTANT THRUST MODES FOR 500 DAY FLIGHTS AND J CAPABILITY OF $20 \text{ M}^2/\text{SEC}^3$

4. J REQUIREMENTS FOR PLANETARY FLIGHT

The accessible regions data given in the previous section are useful in describing generalized interplanetary flight. For missions to particular planets it is more useful to display the trajectory energy requirements as graphs of J vs flight time. The three basic types of missions considered are (1) flyby, (2) parabolic capture, and (3) orbiter. In the flyby mission the vehicle approaches the target planet along a hyperbolic trajectory having a specified miss distance. No constraint is placed upon the approach velocity. In the parabolic capture or rendezvous mission the velocity components of the vehicle and planet are matched at the time of intercept. It is noted that from this parabolic energy condition only a small energy increment is needed to achieve a loosely bound (highly eccentric) capture orbit. As in the flyby mission, any distance of closest approach is possible. In the case of the orbiter mission the vehicle continues thrusting until a circular orbit of specified radius is achieved.

The two phases common to each of the above mission types are the Earth-escape phase (E) and the heliocentric transfer phase (H). A planet-capture phase (C) is added in the case of the orbiter mission. In general, then, the total J requirement and flight time of a mission may be written

$$J = J_E + J_H + J_C \quad (5)$$

$$T_f = T_E + T_H + T_C \quad (6)$$

For preliminary mission analysis, it suffices to treat each phase of the mission as a separate "two-body problem" with the Earth, Sun and target planet as successive central gravitational bodies. Overall results are then pieced together as in the above equations.

Planetocentric Escape and Capture

A constant, tangential thrust program is assumed for the planetocentric phase of flight (Earth-escape and planet-capture). For these phases, the performance difference between the tangential and optimum thrust direction programs is negligible. Furthermore, the tangential thrust assumption allows one to obtain values of (J_E, T_E) and (J_C, T_C) from simple closed-form expressions (Melbourne 1961). This analytical solution has been found to give excellent agreement with results obtained from numerical integration solutions of the escape and capture trajectories.

Figure 10 shows the J requirement for Earth-escape from initial circular orbits of 200, 1000 and 2000 N. miles altitude. These results apply specifically to the constant acceleration mode of operation. As it turns out, the J vs T curve for planetocentric escape or capture is only weakly dependent upon the mode of thruster operation, i.e., the constant acceleration and constant thrust curves are very nearly the same. Thus, for example, in the case of a constant acceleration program, the acceleration (a) would appear as a parameter along this curve according to the relation $a^2 T_E = J_E$.

In the case of a constant thrust program, points along this curve could be identified with the parameters - initial acceleration (a_0) and specific impulse (I_{SP}).

The J requirements for capture into a circular orbit at 3 planet radii are shown in Figure 11 for each of the planets. The ordering of capture requirements essentially follows the ordering of planetary masses. For typical acceleration levels appropriate to each planetary mission, the capture times range from 12 days (Mercury) to 430 days (Jupiter). The corresponding J requirements range from 2.3 to $14 \text{ m}^2/\text{sec}^3$.

Heliocentric Transfer Phase

Requirements of the heliocentric transfer between Earth and the target planet are found from numerical integration solutions which assume an optimum thrust program and an optimum Earth-position at launch. Generally, a coast period is included in the heliocentric transfer. Since we are mainly interested in the total J and flight time requirements of a mission, graphs of J vs T will not be given separately for the heliocentric transfer phase.

Total J Requirements - Constant Thrust Mode

With reference to Equations (5) and (6), it is seen that, if one wishes to minimize the total J required for a given total flight time, there arises the problem of optimum allocation of effort (J, T) between the various mission phases. Given the basic data for each of the phases, this problem is

readily solved (e.g., by variation of parameters and graphical plots). Results to be presented assume the constant thrust mode of propulsion with an optimum specific impulse chosen for each mission and flight time. Although the minimum J solutions for constant thrust operation do depend upon the parameters (a_0 and I_{sp}) of the propulsion system, this dependence is very weak over the parameter range of typical electric propulsion systems. Hence, to a good degree of approximation, the following results apply generally to constant thrust operation when the specific impulse is optimized.

Figures 12 through 14 summarize the total J requirements as a function of total flight time for flyby, capture and orbiter missions to Mercury, Venus and Mars. Similar information is presented in Figures 15 through 17 for missions to the outer planets. In all cases an Earth-escape phase from a 1000 N.mile orbit is assumed. The orbiter missions terminate in a circular orbit about the target planet at a distance of 3 planet radii from the center. For simplicity, the effect of the planetary

eccentricities on the J requirement has not been taken into account. A circular planetary orbit at mean distance from the Sun is assumed for all the planets except Mercury (aphelion encounter) and Pluto (perihelion encounter).

A significant characteristic of these results is that, in general, the longer the time allowed to reach a given planet, the smaller the J requirement. One notes, however, that the J requirement levels off beyond some flight time so that an extended flight time tends to give diminishing returns. This point usually occurs when the heliocentric travel angle of the trajectory becomes quite large (about 270°).

Figures 12 through 14 show, for a typical J capability of $30 \text{ m}^2/\text{sec}^3$, flight times to the inner or terrestrial planets ranging from 100 days for a Venus flyby to 300 days for a Mercury orbiter. Similarly, from Figures 15 through 17, flight times to the outer planets range from 450 days for a Jupiter flyby to 2950 days for a Neptune orbiter.

One notes from Figures 14 through 17 that the Pluto and Neptune missions require very nearly the same flight times. This is due to the assumed perihelion encounter with Pluto at which time the radial distances of the two planets from the Sun are about the same. The 15° latitude of Pluto at this time would impose a severe penalty on ballistic flights, but imposes a negligible penalty on thrusting flights.

It is sometimes convenient to display the J vs T results for each planet separately so that one can easily

measure the relative increase in requirements as the mission mode goes from flyby to capture to orbiter. This is shown in Figures 18 through 25. For example, Figure 18 shows that in the case of Mercury missions there is a large difference in either J or flight time between the flyby and capture flights but little difference between the capture and orbiter flights. Figure 21 shows the opposite characteristic for missions to Jupiter. These results are due, of course, to the relative importance of the planetary velocities and masses.

As an example of the desirable range of specific impulse, the electric spacecraft having a propulsion/vehicle constraint of $a_0 I_{SP} = 5.4$ m/sec would require a minimum I_{SP} of about 3000 seconds for the Venus flyby and a maximum I_{SP} of about 18,000 seconds for the Pluto orbiter. This is a reasonable range of I_{SP} for ion engines, although power efficiency does fall off rapidly at the lower end of this range. Table 1 illustrates a phase requirement breakdown for a Mercury orbiter mission of 253 days duration.

One final point concerns the magnitude of the approach velocity for the minimum J flyby missions. Recall that no constraint is placed upon this velocity. Table 2 lists the approach hyperbolic velocities for each of the planets over the range of flight times indicated in Figures 12 and 15. In general, the shorter the flight time the higher the velocity. It is seen that even for the longer flights of interest the approach velocity remains quite high except for Venus and Mars

flybys. This is especially true for the outer planet flybys where velocities above 20 km/sec are typical. It is quite possible that mission constraints may require a certain amount of velocity reduction. In this case, the J requirement would lie somewhere between that of the minimum J flyby and the parabolic capture missions.

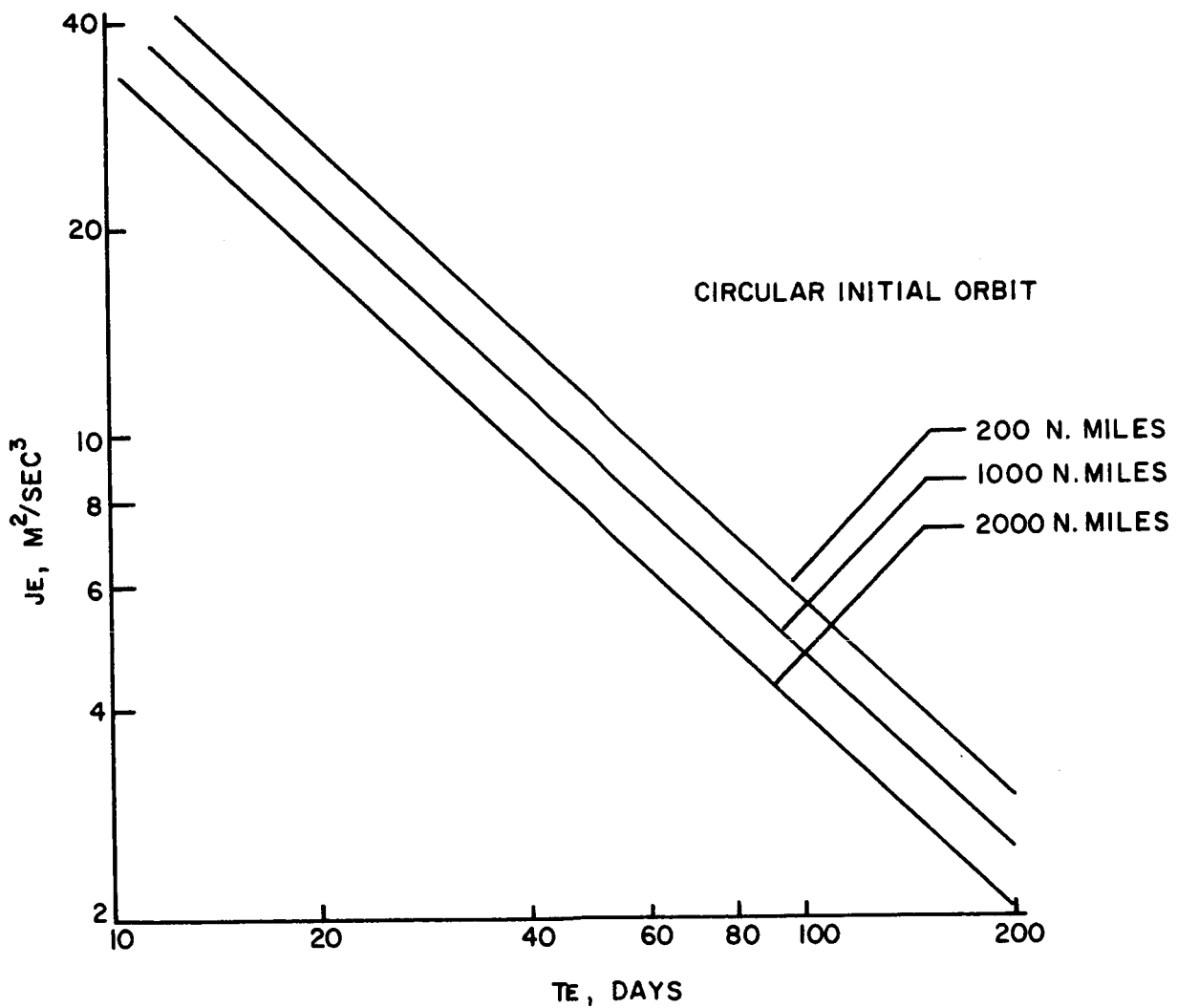


FIGURE 10. EARTH ESCAPE REQUIREMENTS, CONSTANT ACCELERATION MODE, $J_E = a^2 T_E$

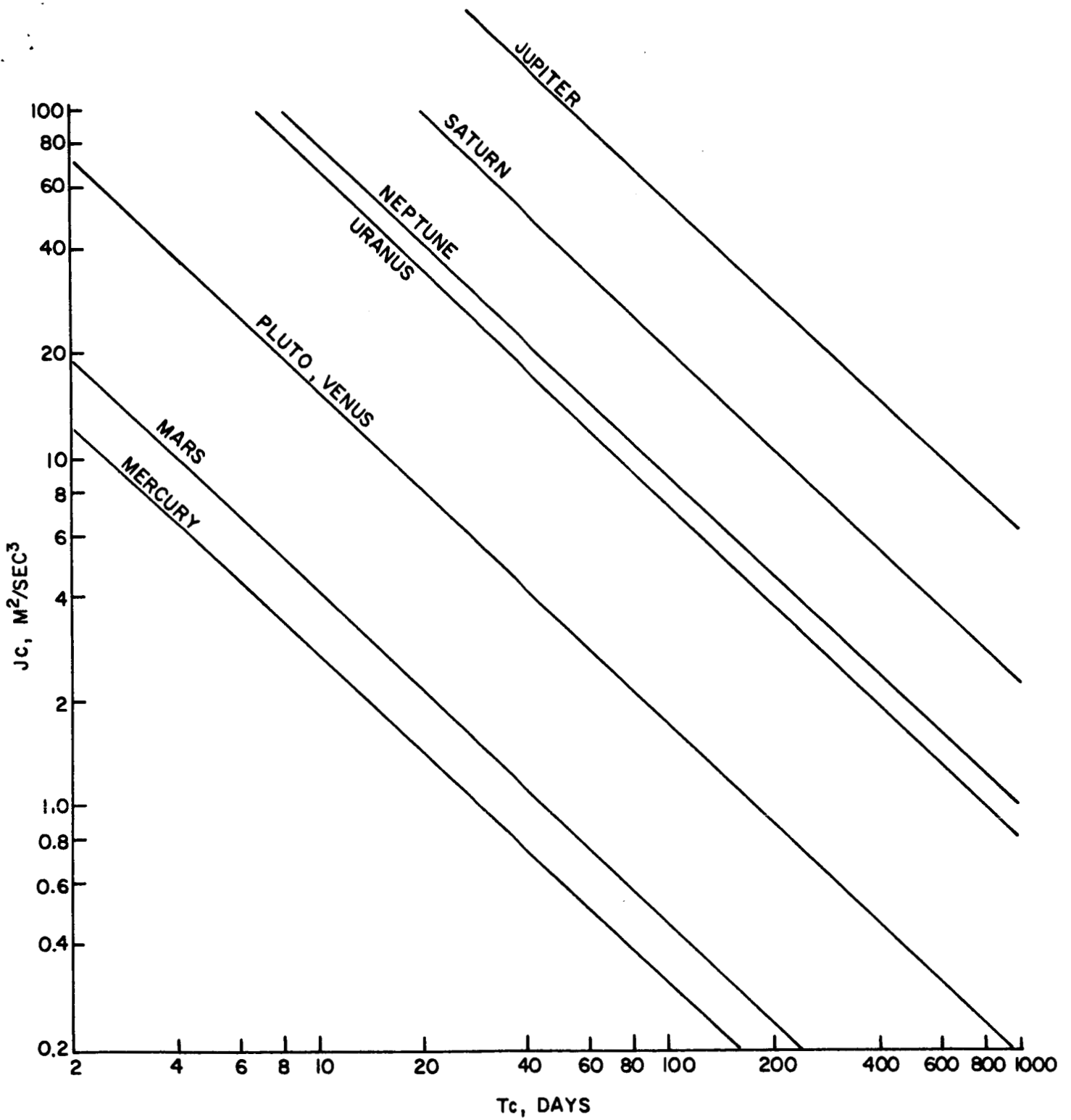


FIGURE II. PLANET - CAPTURE REQUIREMENTS FOR CIRCULAR ORBIT AT THREE PLANET RADII, CONSTANT ACCELERATION MODE, $J_c = a^2 T_c$

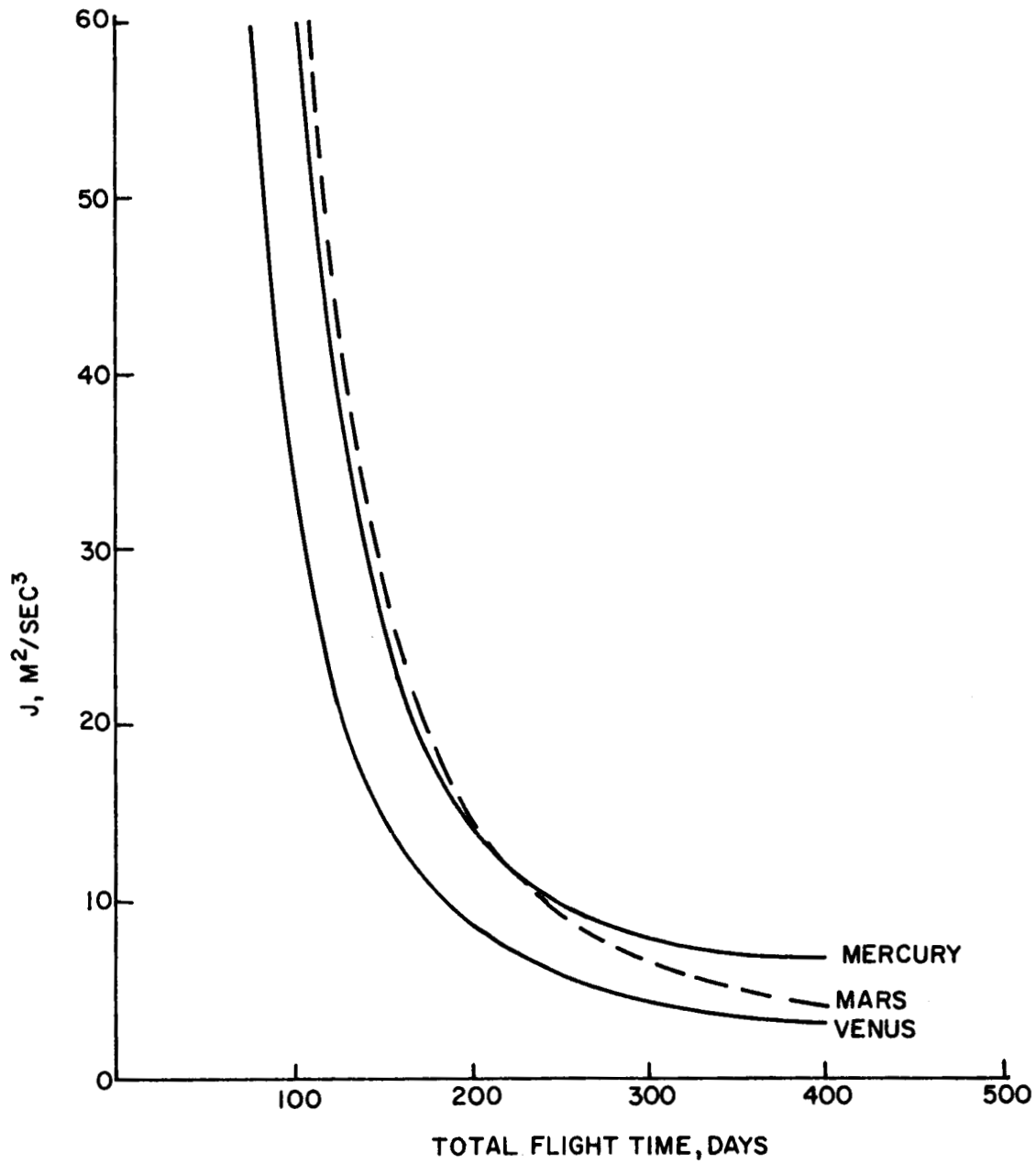


FIGURE 12. J REQUIREMENTS FOR FLY-BY MISSIONS TO THE INNER PLANETS, EARTH ESCAPE FROM 1000 N. MILE ORBIT, CONSTANT THRUST MODE WITH OPTIMUM SPECIFIC IMPULSE

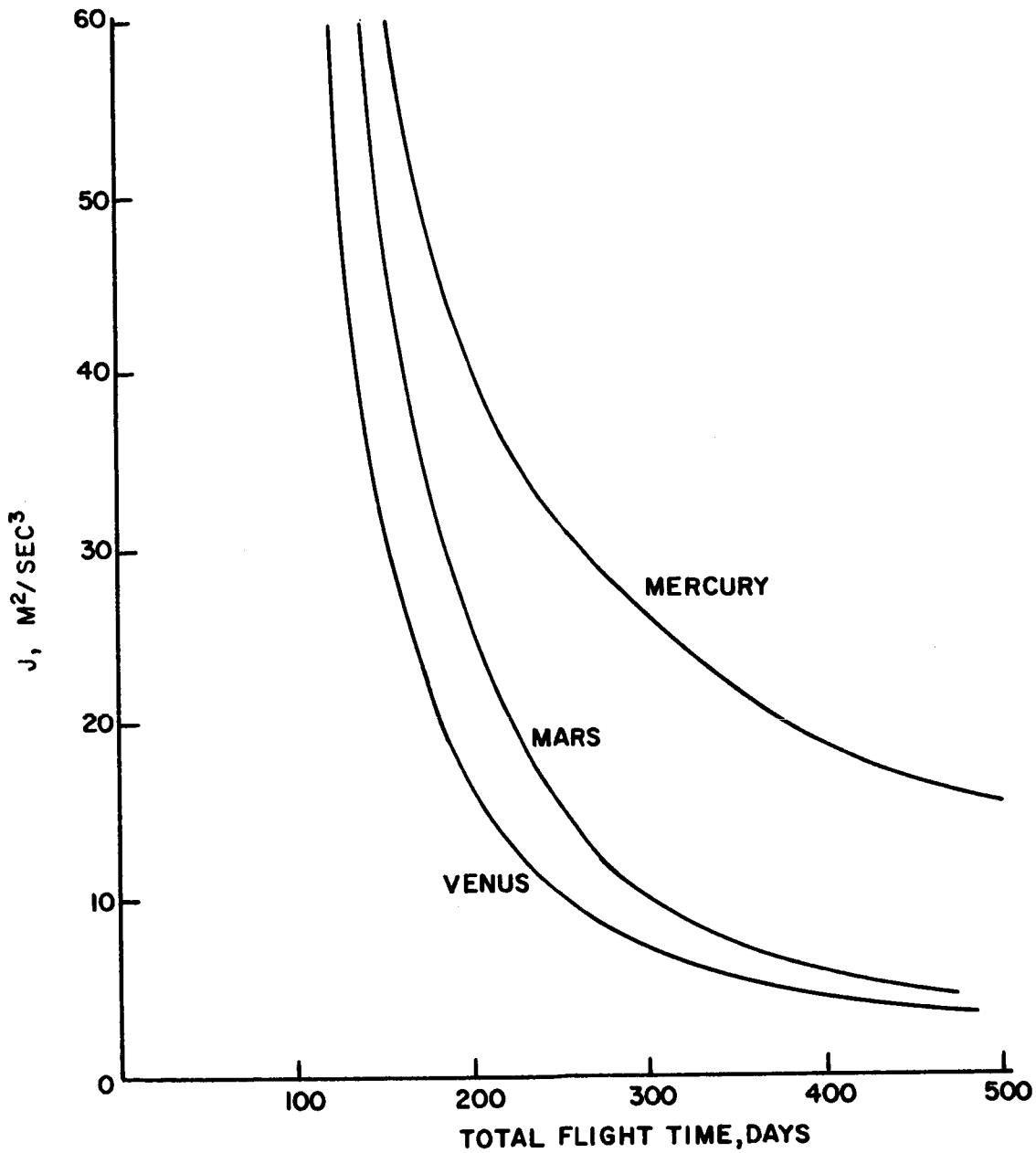


FIGURE 13. J REQUIREMENTS FOR PARABOLIC CAPTURE MISSIONS TO THE INNER PLANETS, EARTH ESCAPE FROM 1000 N. MILE ORBIT, CONSTANT THRUST MODE WITH OPTIMUM SPECIFIC IMPULSE

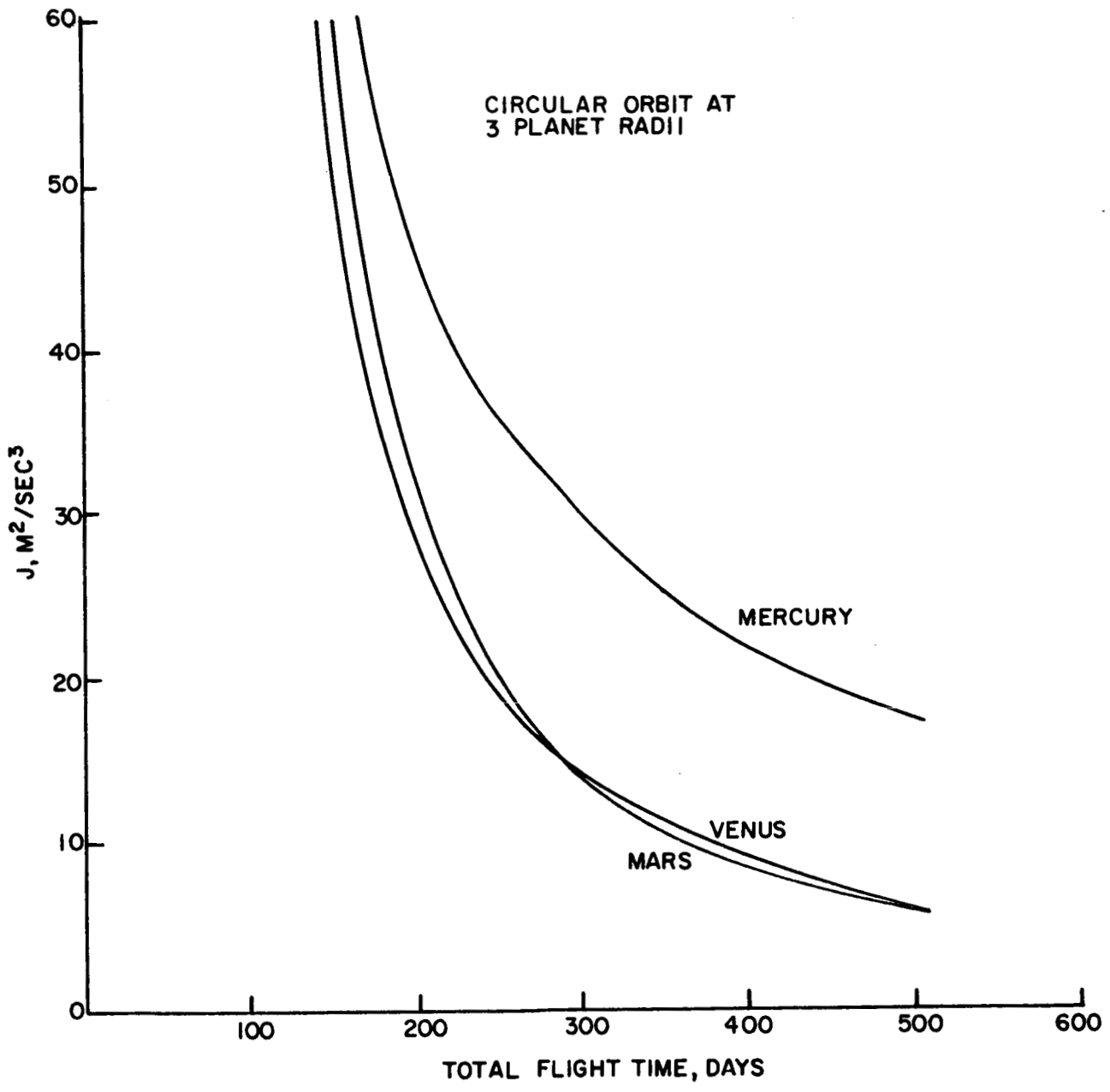


FIGURE 14. J REQUIREMENTS FOR ORBITER MISSIONS TO THE INNER PLANETS, EARTH ESCAPE FROM 1000 N. MILE ORBIT, CONSTANT THRUST MODE WITH OPTIMUM SPECIFIC IMPULSE

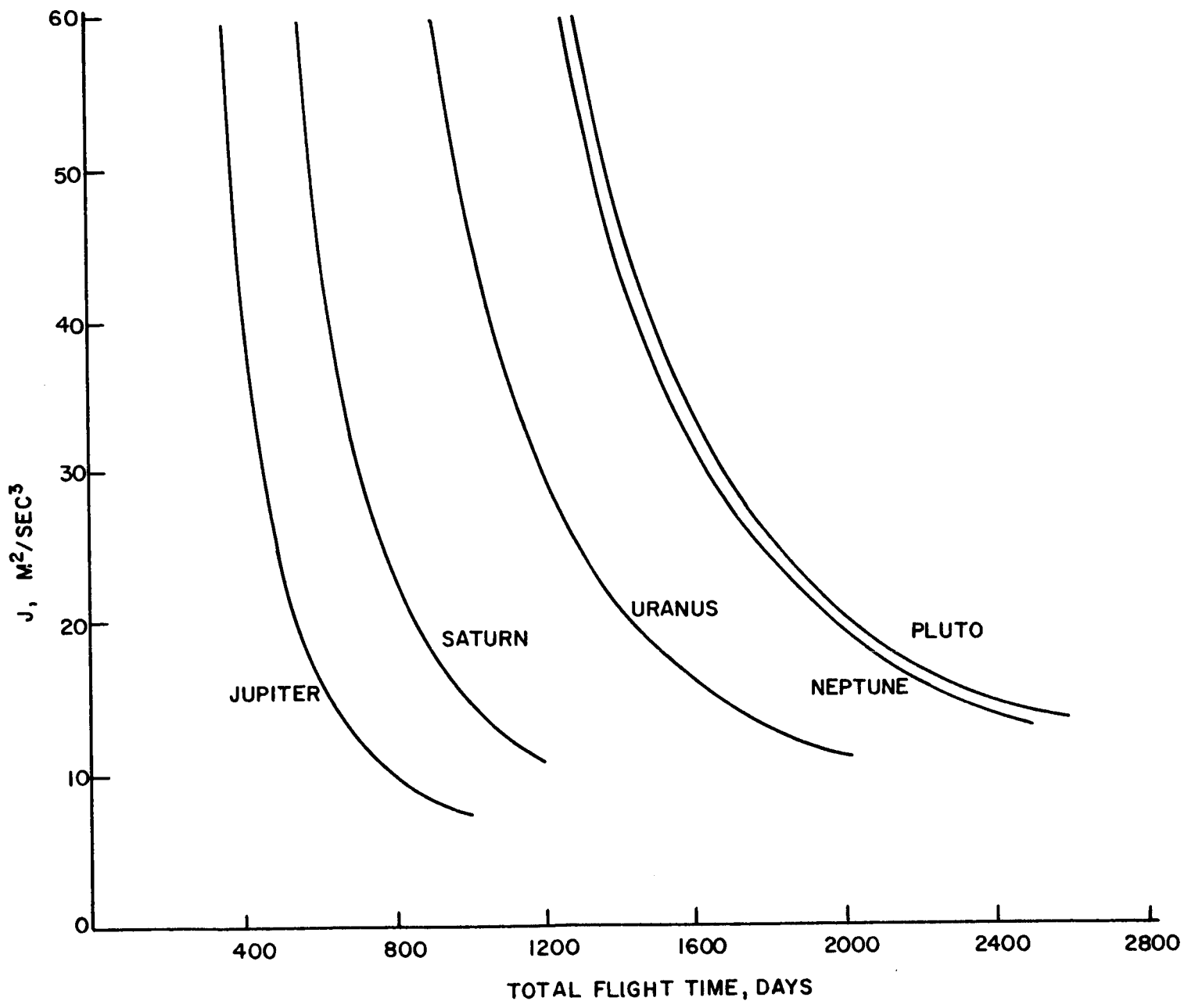


FIGURE 15. J REQUIREMENTS FOR FLY-BY MISSIONS TO THE OUTER PLANETS, EARTH ESCAPE FROM 1000 N. MILE ORBIT, CONSTANT THRUST MODE WITH OPTIMUM SPECIFIC IMPULSE

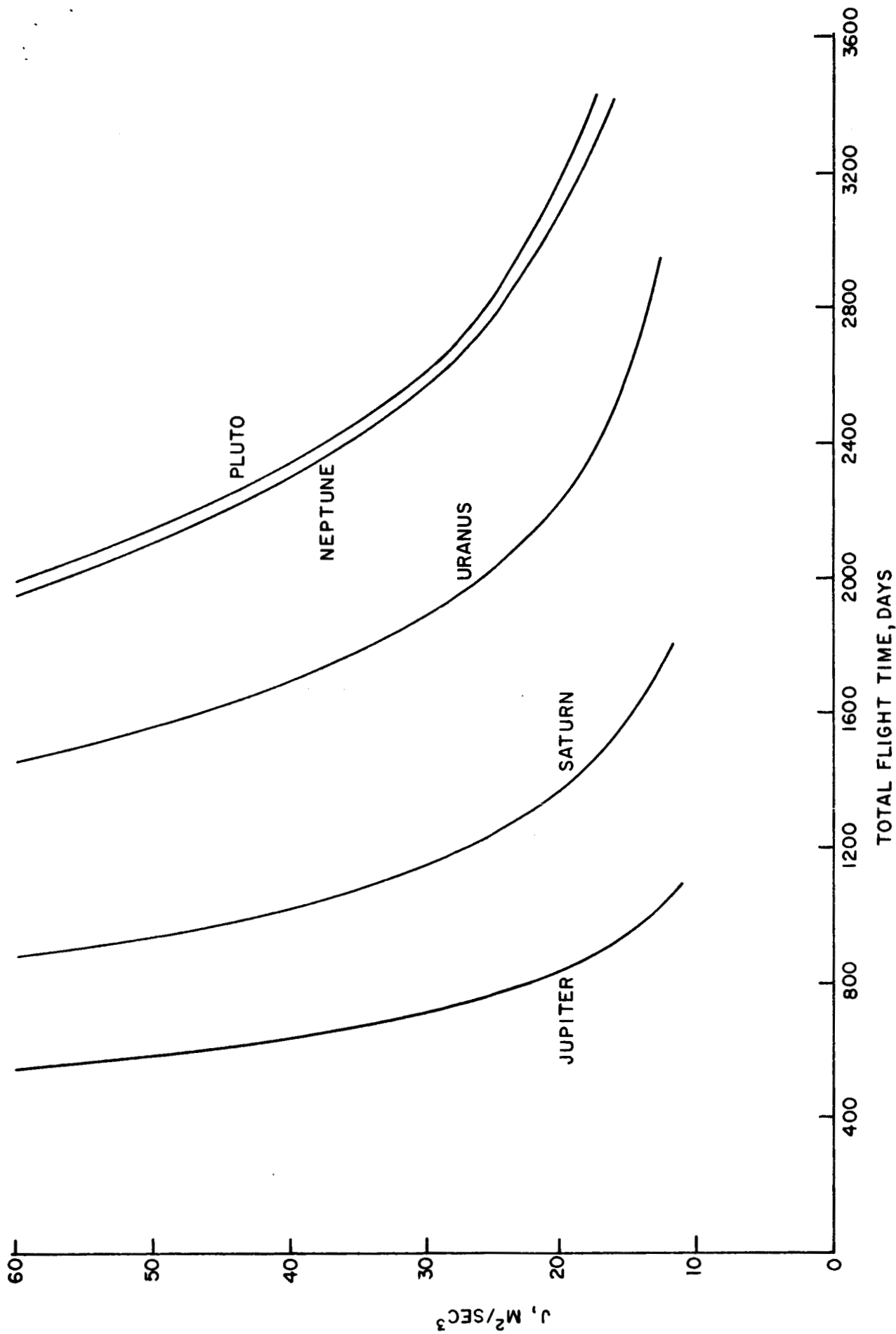


FIGURE 16. J REQUIREMENTS FOR PARABOLIC CAPTURE MISSIONS TO THE OUTER MISSIONS, EARTH ESCAPE FROM 1000 N. MILE ORBIT, CONSTANT THRUST MODE WITH OPTIMUM SPECIFIC IMPULSE.

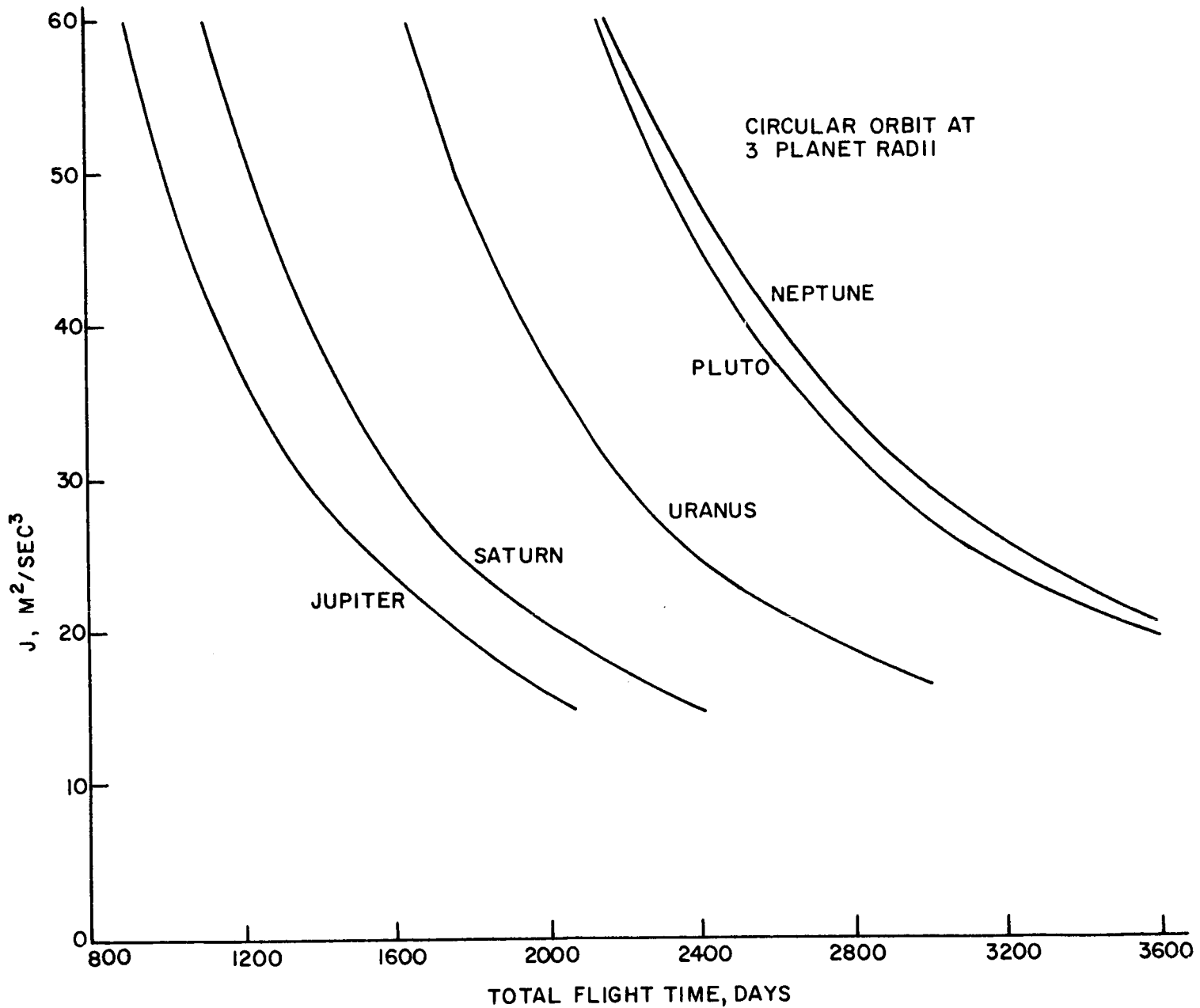


FIGURE 17. J REQUIREMENTS FOR ORBITER MISSIONS TO THE OUTER PLANETS, EARTH ESCAPE FROM 1000 N. MILE ORBIT, CONSTANT THRUST MODE WITH OPTIMUM SPECIFIC IMPULSE

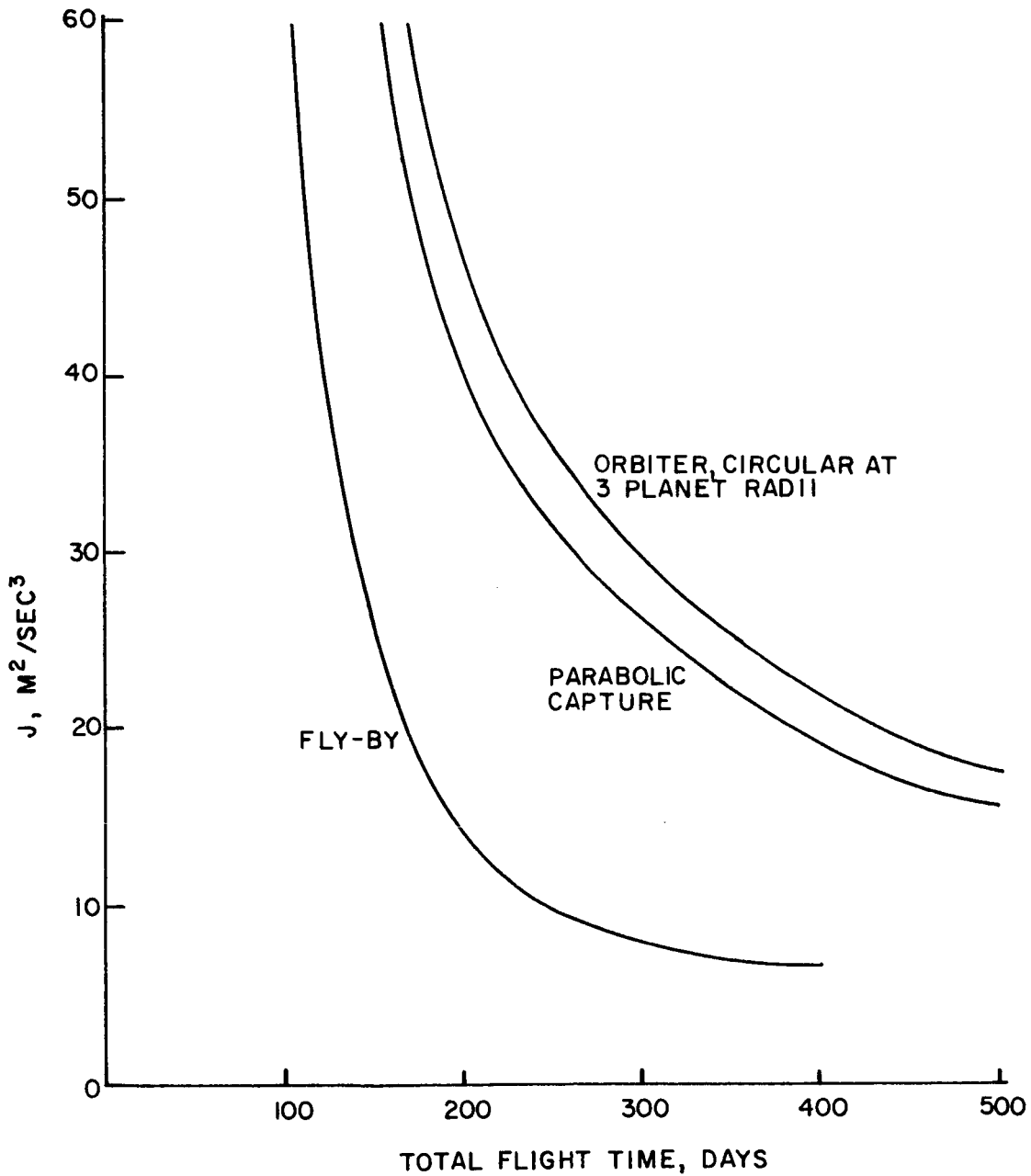


FIGURE 18. J REQUIREMENTS FOR MISSIONS TO MERCURY, EARTH ESCAPE FROM 1000 N. MILE ORBIT, CONSTANT THRUST MODE WITH OPTIMUM SPECIFIC IMPULSE.

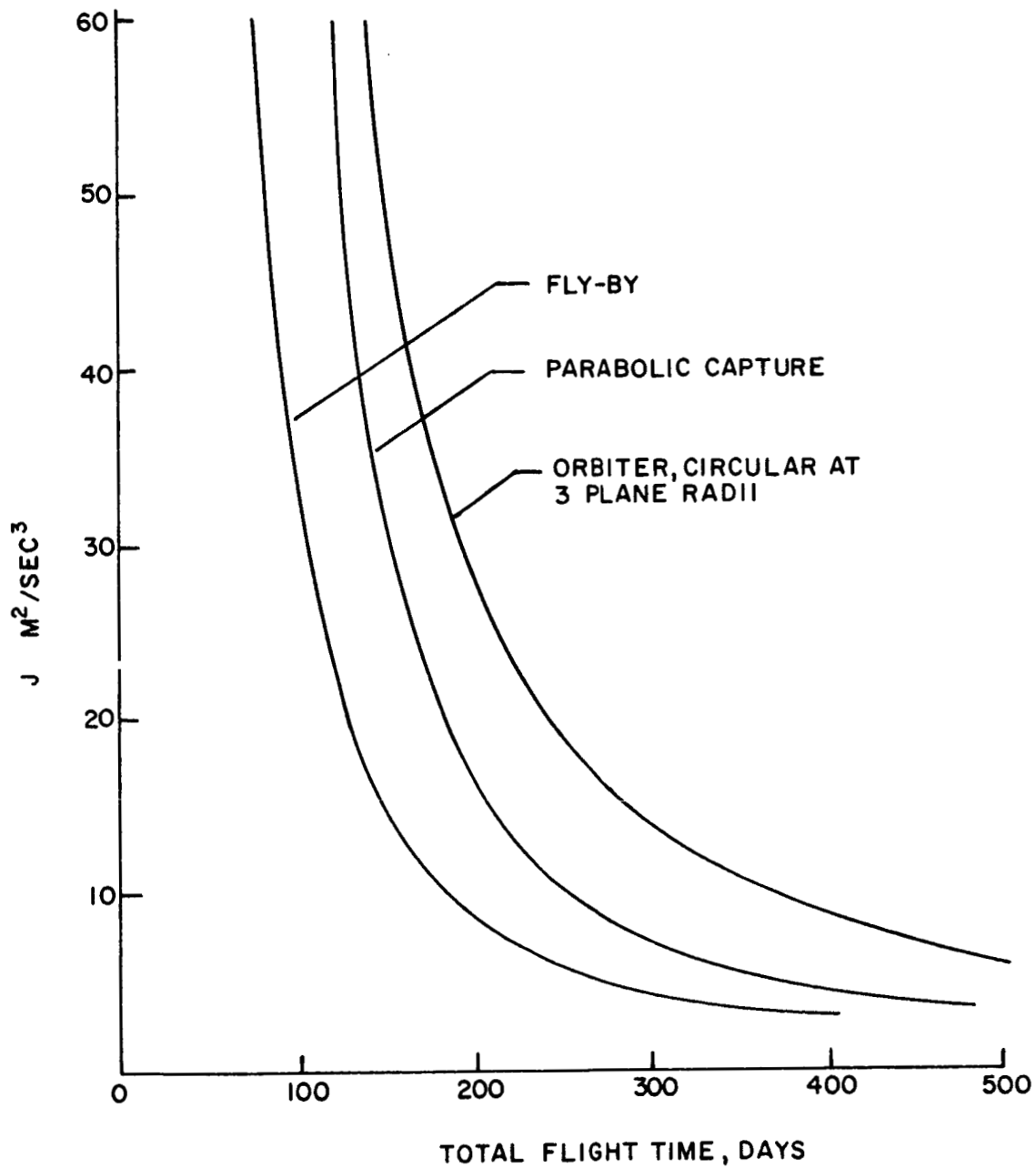


FIGURE 19. J REQUIREMENTS FOR MISSIONS TO VENUS, EARTH ESCAPE FROM 1000 N. MILE ORBIT, CONSTANT THRUST MODE WITH OPTIMUM SPECIFIC IMPULSE.

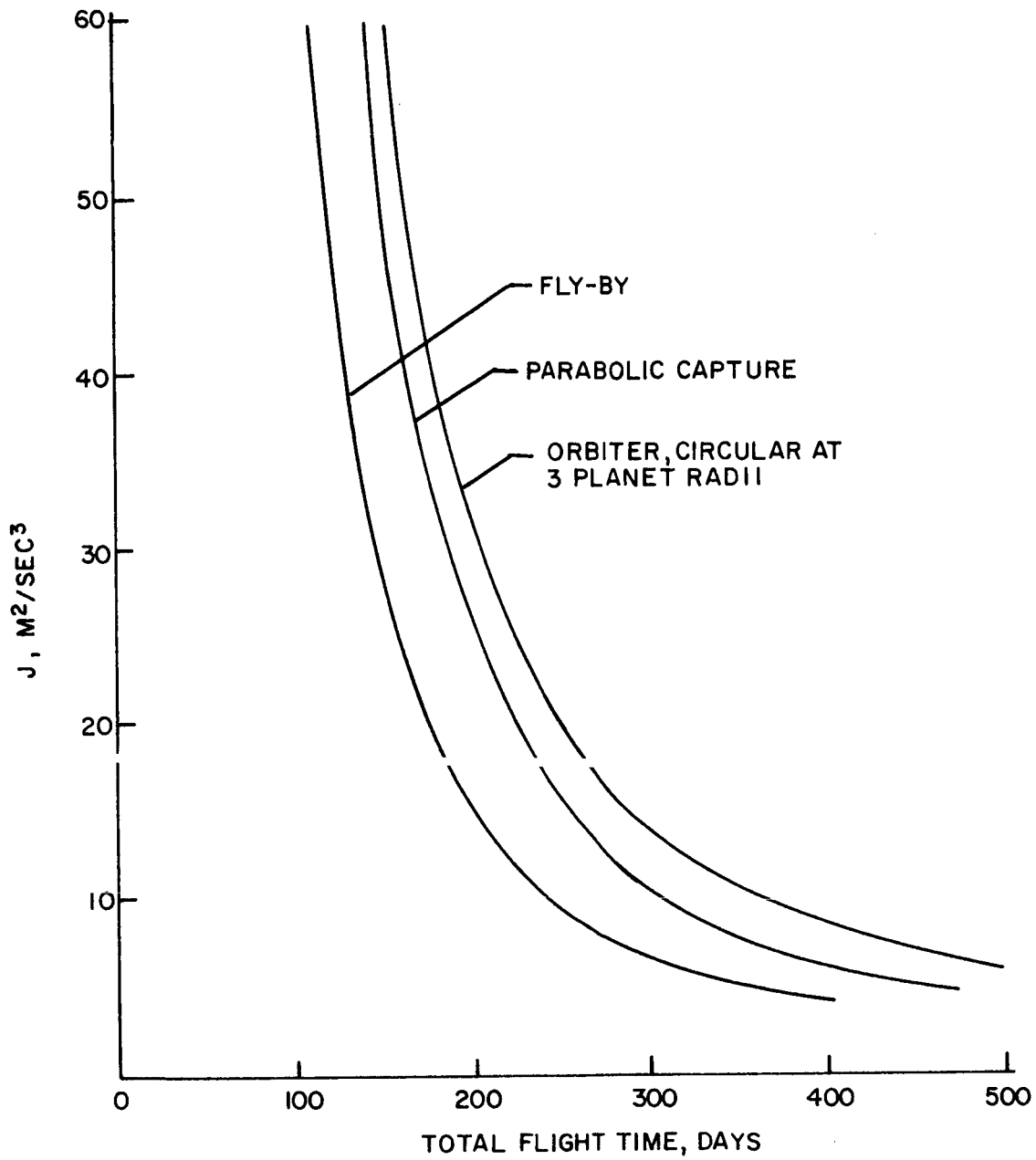


FIGURE 20. J REQUIREMENTS FOR MISSIONS TO MARS, EARTH ESCAPE FROM 1000 N. MILE ORBIT, CONSTANT THRUST MODE WITH OPTIMUM SPECIFIC IMPULSE

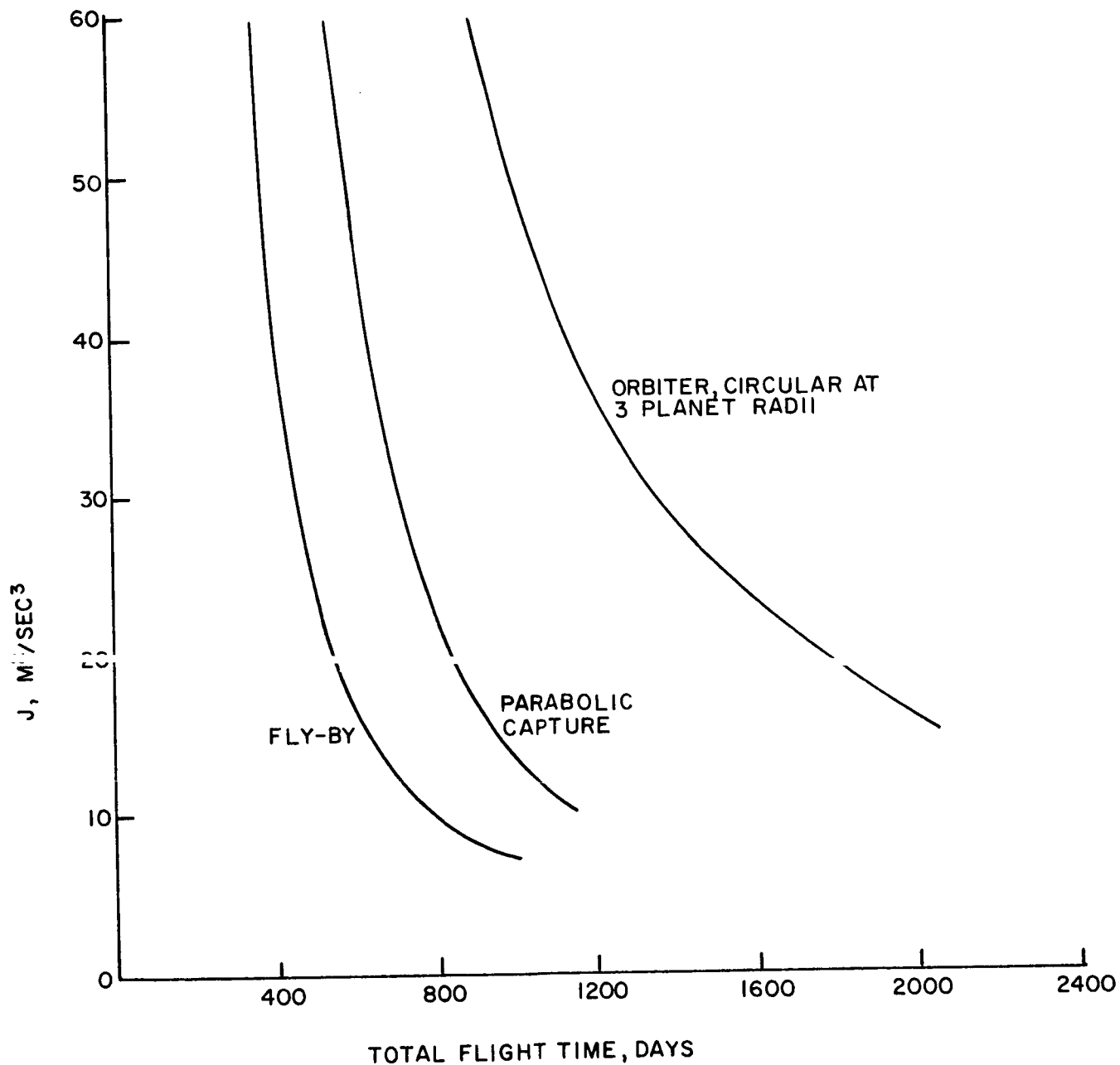


FIGURE 21. J REQUIREMENTS FOR MISSIONS TO JUPITER, EARTH ESCAPE FROM 1000 N. MILE ORBIT, CONSTANT THRUST MODE WITH OPTIMUM SPECIFIC IMPULSE.

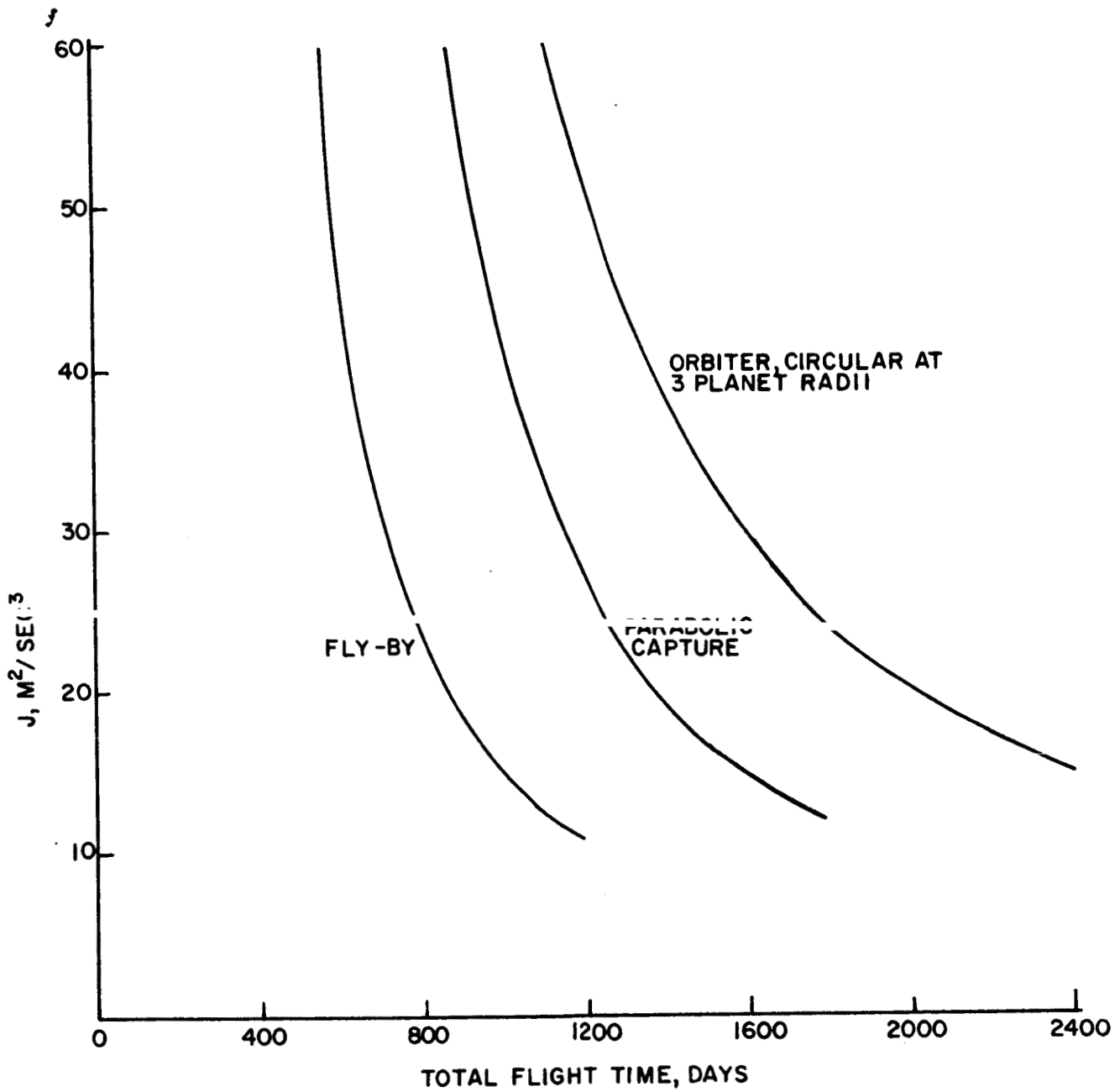


FIGURE 22. J REQUIREMENTS FOR MISSIONS TO SATURN, EARTH ESCAPE FROM 1000 N. MILE ORBIT, CONSTANT THRUST MODE WITH OPTIMUM SPECIFIC IMPULSE.

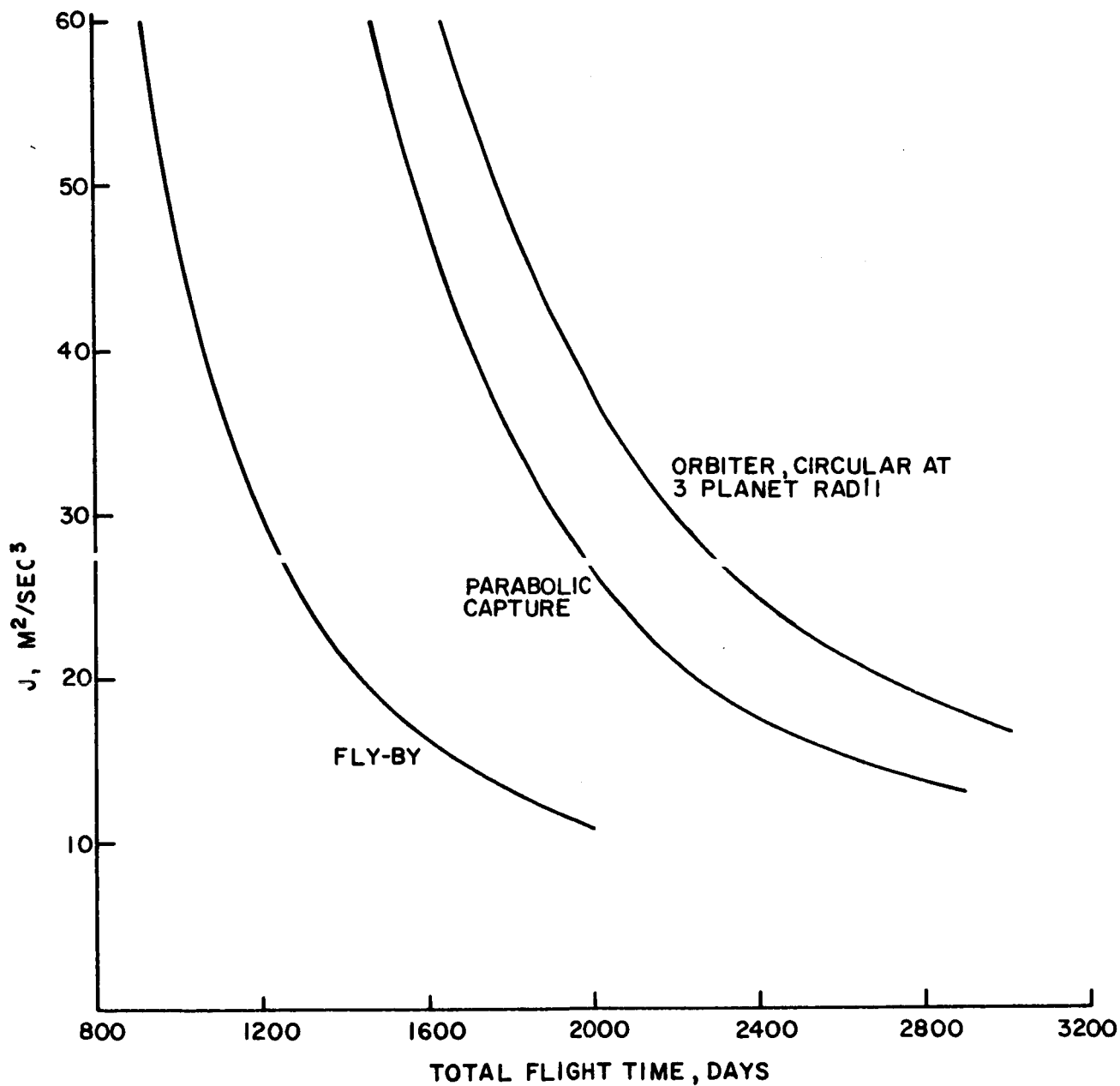


FIGURE 23. J REQUIREMENTS FOR MISSIONS TO URANUS, EARTH ESCAPE FROM 1000 N. MILE ORBIT, CONSTANT THRUST MODE WITH OPTIMUM SPECIFIC IMPULSE

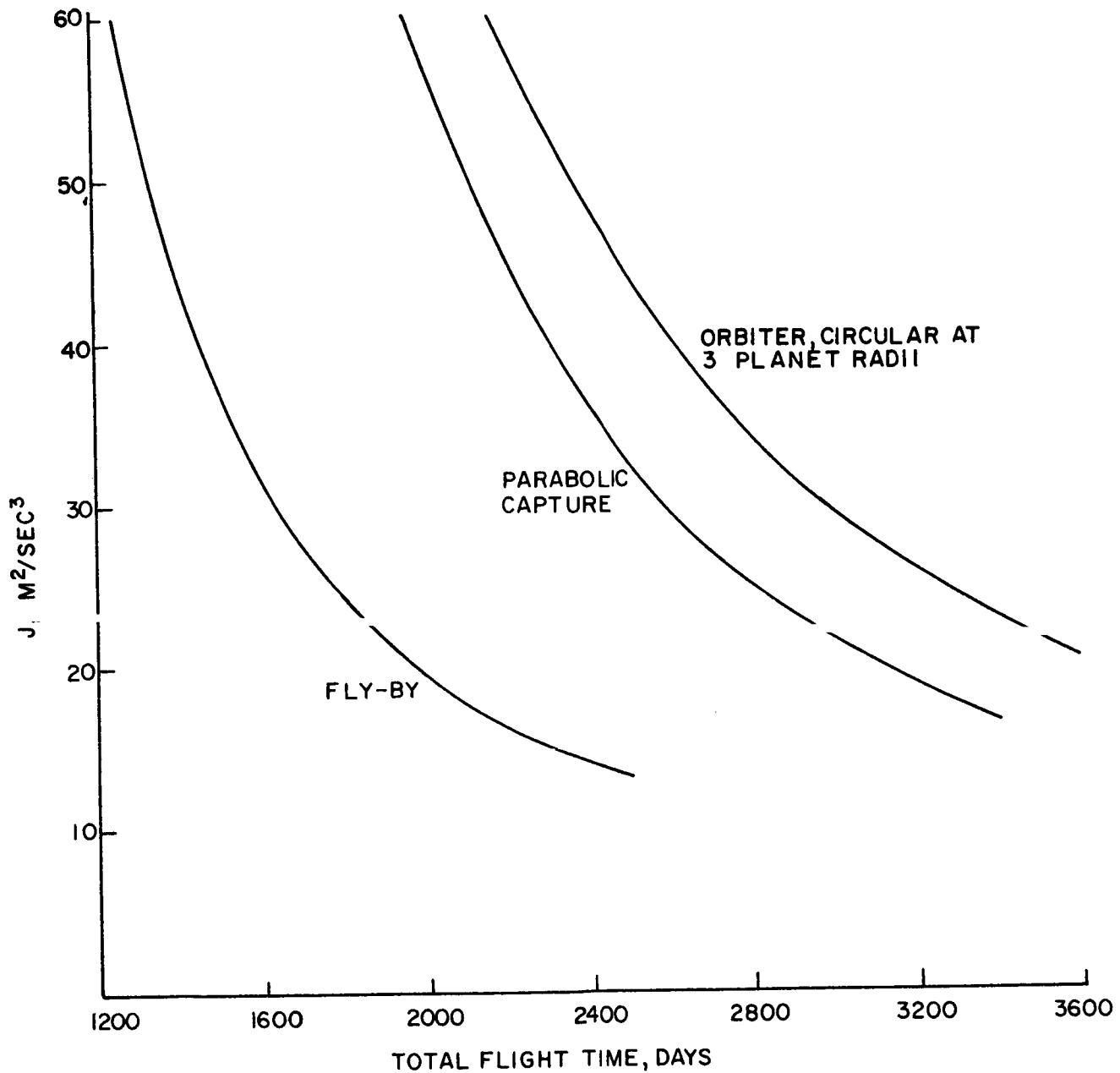


FIGURE 24. J REQUIREMENTS FOR MISSIONS TO NEPTUNE, EARTH ESCAPE FROM 1000 N. MILE ORBIT, CONSTANT THRUST MODE WITH OPTIMUM SPECIFIC IMPULSE

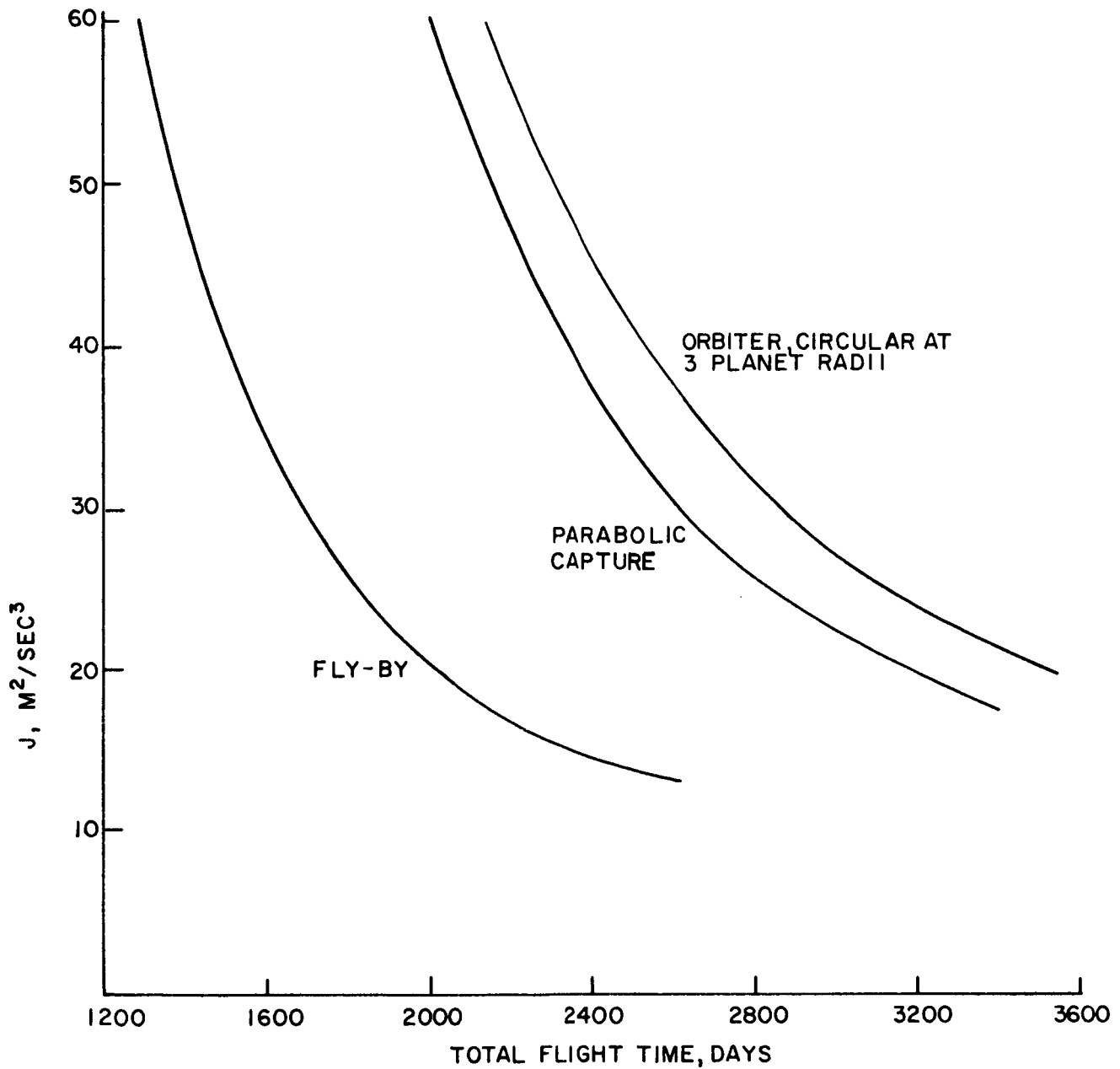


FIGURE 25. J REQUIREMENTS FOR MISSIONS TO PLUTO, EARTH ESCAPE FROM 1000 N. MILE ORBIT, CONSTANT THRUST MODE WITH OPTIMUM SPECIFIC IMPULSE

Table 1

PHASE BREAKDOWN OF A TYPICAL ORBITER MISSION
TO MERCURY

- Constant thrust mode, $a_0 I_{SP} = 5.4 \text{ m/sec}$
- Earth-escape from 1000 N. mile circular orbit
- Circular orbit at Mercury - 3 Mercury radii
- Optimum $I_{SP} = 5000 \text{ seconds}$

Mission Phase	a_0 m/sec ²	J m ² /sec ³	T days	Coast Period days
Earth-escape	1.08×10^{-3}	7.2	63	0
Heliocentric transfer	1.23×10^{-3}	25.7	180	42
Mercury- capture	1.75×10^{-3}	2.8	10	0
Total		35.7	253	42

Table 2

RANGE OF APPROACH HYPERBOLIC VELOCITIES
FOR MINIMUM J FLYBY MISSIONS

<u>Planet</u>	<u>Approach Velocity, km/sec</u>
Mercury	11-27
Venus	3-20
Mars	2-20
Jupiter	10-36
Saturn	15-45
Uranus	24-55
Neptune	29-63
Pluto	29-63

Note: The higher approach velocities correspond to the shorter flight times.

5. EXAMPLES OF PAYLOAD CAPABILITY

The generalized trajectory energy requirements given in the preceding sections may be translated into payload numbers via the expressions (2) to (4). Two conceptual nuclear-electric spacecraft are assumed for illustrative purposes. Figure 26 shows the payload vs J curves for the two spacecraft designated NES-1 and NES-2. Each spacecraft has an assumed powerplant weight of 10,000 lb. Structure and tankage weights are estimated, respectively, as 10 percent of the powerplant weight and 5 percent of the maximum propellant loading. Guidance and control equipment and propellant reserves are assumed to be 1000 lb. The C&E (communications and experiments) payload is defined as the net payload (M_{PL}) less the weight of structure, tankage, and guidance and control.

The NES-1 spacecraft, which could be placed into Earth orbit by the Saturn 1B launch vehicle, has an initial weight of 20,000 lb and operates at a power rating of 240 kwj ($\alpha_j = 41.6 \text{ lb/kwj}$). The 30,000 lb NES-2 spacecraft is assumed to operate at a higher power of 400 kwj ($\alpha_j = 25 \text{ lb/kwj}$). Considering the different capabilities of the two spacecraft, minimum C&E payloads of 500 lb and 2000 lb are chosen. These payloads then determine the maximum J capabilities of the NES-1 and NES-2 spacecraft as $29 \text{ m}^2/\text{sec}^3$ and $55.5 \text{ m}^2/\text{sec}^3$, respectively. It should be noted that even the higher value of α_j assumed here is considered somewhat optimistic for current designs of nuclear-electric powerplants.

Figure 27 shows a 380 and 600 day flight time contour for the low-thrust NES-1 spacecraft delivering a 500 lb C&E payload. For comparison purposes, similar contours are given for a ballistic spacecraft launched by the Saturn 1B-Centaur vehicle. In the ballistic case, the C&E payload is taken as 25 percent of the total spacecraft weight at launch. For a maximum flight time of 380 days, the performance of the low-thrust vehicle is somewhat better for out-of-the-ecliptic flights and close flybys of the Sun. In general, however, the performance advantage for short flights is either marginal or nonexistent. The 600 day flight shows off the low-thrust stage to better advantage, especially for out-of-the-ecliptic missions. Still, neither vehicle can extend the planetary flybys to Saturn or beyond in trips of 600 days or less.

Figure 28 compares the NES-2 and Saturn V-Centaur for a 2000 lb C&E payload. In this case the accessible regions performance of the low-thrust vehicle is superior in all respects for the longer flight times. For a flight time limitation of 570 days, the exploration capability extends from an "over-the-Sun" flight at 1.5 AU to the planet Saturn. 1100 day flights enlarge this region to 10 AU above the Sun and beyond the planet Uranus. The advantage of the low-thrust vehicle in this comparison would be reduced somewhat with the choice of a smaller payload. Also, the use of the planet Jupiter as a gravity-assist body can extend the region accessible to the ballistic spacecraft.

The flight time performance of the two conceptual nuclear-electric spacecraft for planetary exploration is listed in Tables 3 and 4. The range of C&E payload considered is 500-2000 lb for the NES-1 spacecraft and 2000-8000 lb for the NES-2 spacecraft. For example, consider the case of missions to Jupiter with the NES-1 spacecraft. The flight times required to deliver a 500 lb payload are 460 days for the flyby missions, 720 days for the minimal capture missions, and 1390 days for the circular (3 radii) orbiter mission. The flight times required to deliver a 2000 lb payload on these missions are 530, 830, and 1740 days, respectively. The rather low sensitivity of flight time to payload is to be noted. In general, the ratio $\Delta(\text{flight time})/\Delta(\text{payload})$ is of the order 1/3.

SPACECRAFT PARAMETERS

INITIAL WEIGHT
 POWER PLANT WEIGHT
 STRUCTURE, TANKAGE, G & C
 KINETIC (JET) POWER
 SPECIFIC WEIGHT

NES-1

20,000 LB.
 10,000 LB.
 2400 LB.
 240 KW.
 41.6 LB./KW

NES-2

30,000 LB.
 10,000 LB.
 3500 LB.
 400 KW.
 25 LB./KW

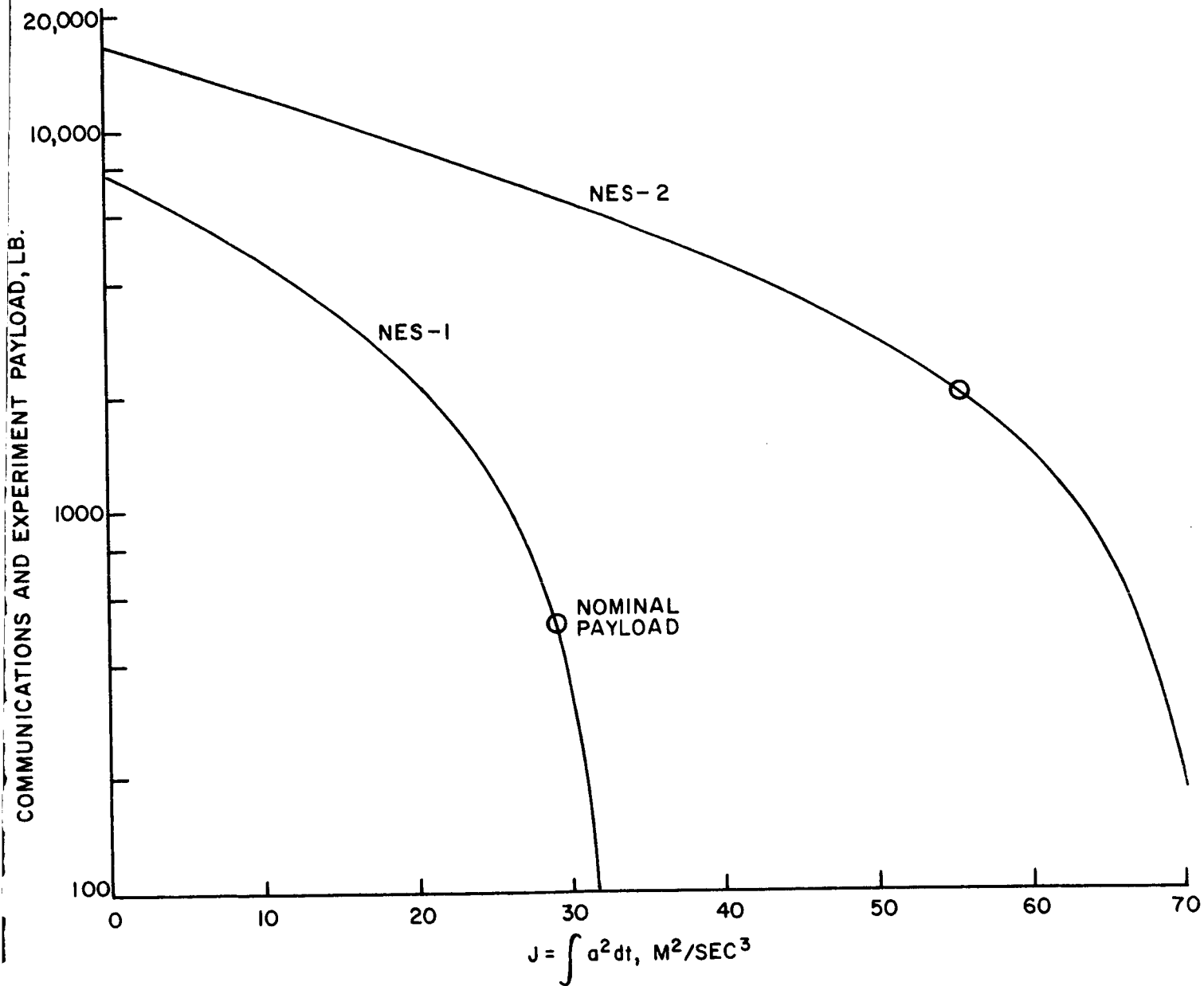


FIGURE 26. PERFORMANCE CURVES FOR TWO CONCEPTUAL DESIGNS OF NUCLEAR-ELECTRIC SPACECRAFT.

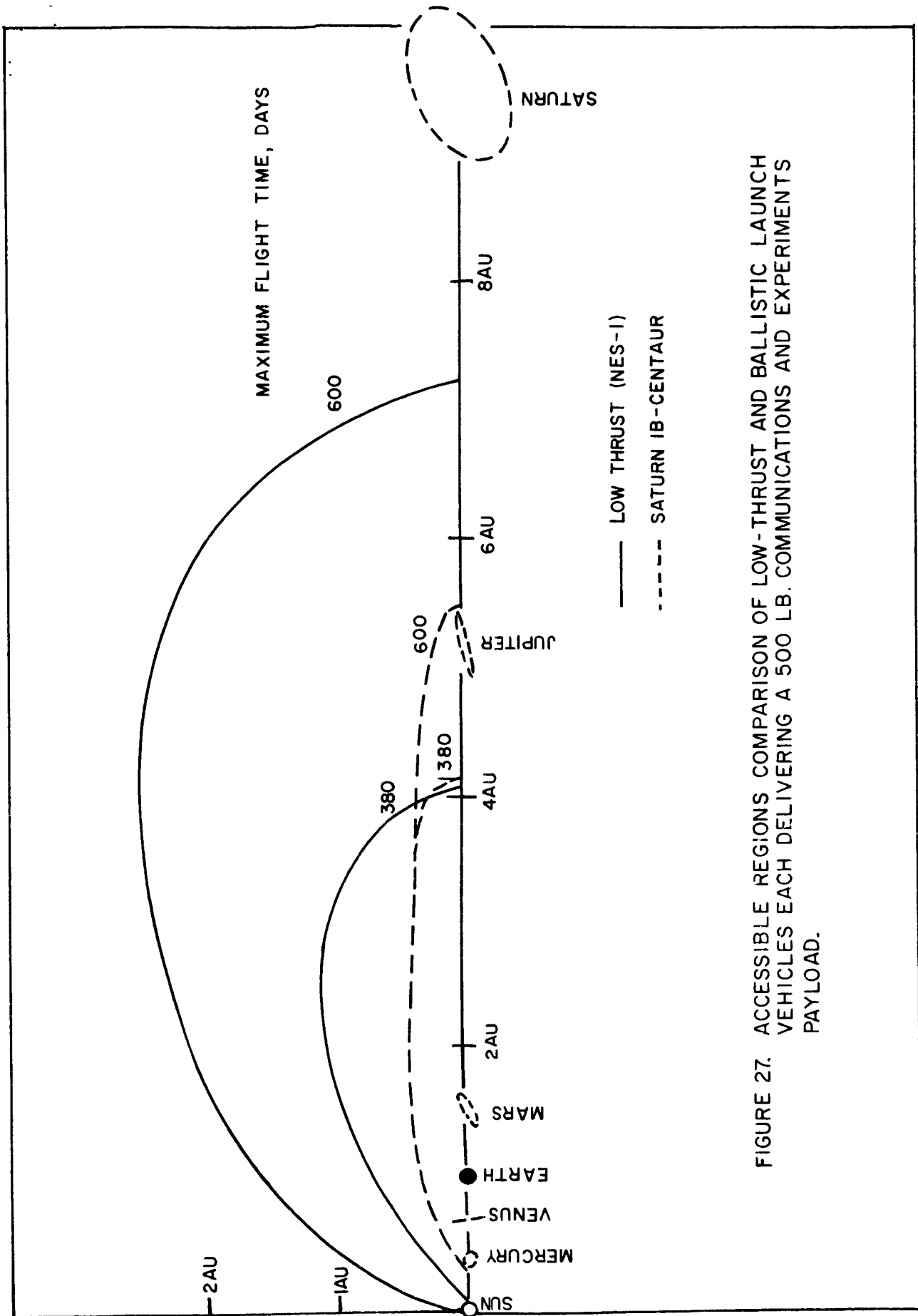


FIGURE 27. ACCESSIBLE REGIONS COMPARISON OF LOW-THRUST AND BALLISTIC LAUNCH VEHICLES EACH DELIVERING A 500 LB. COMMUNICATIONS AND EXPERIMENTS PAYLOAD.

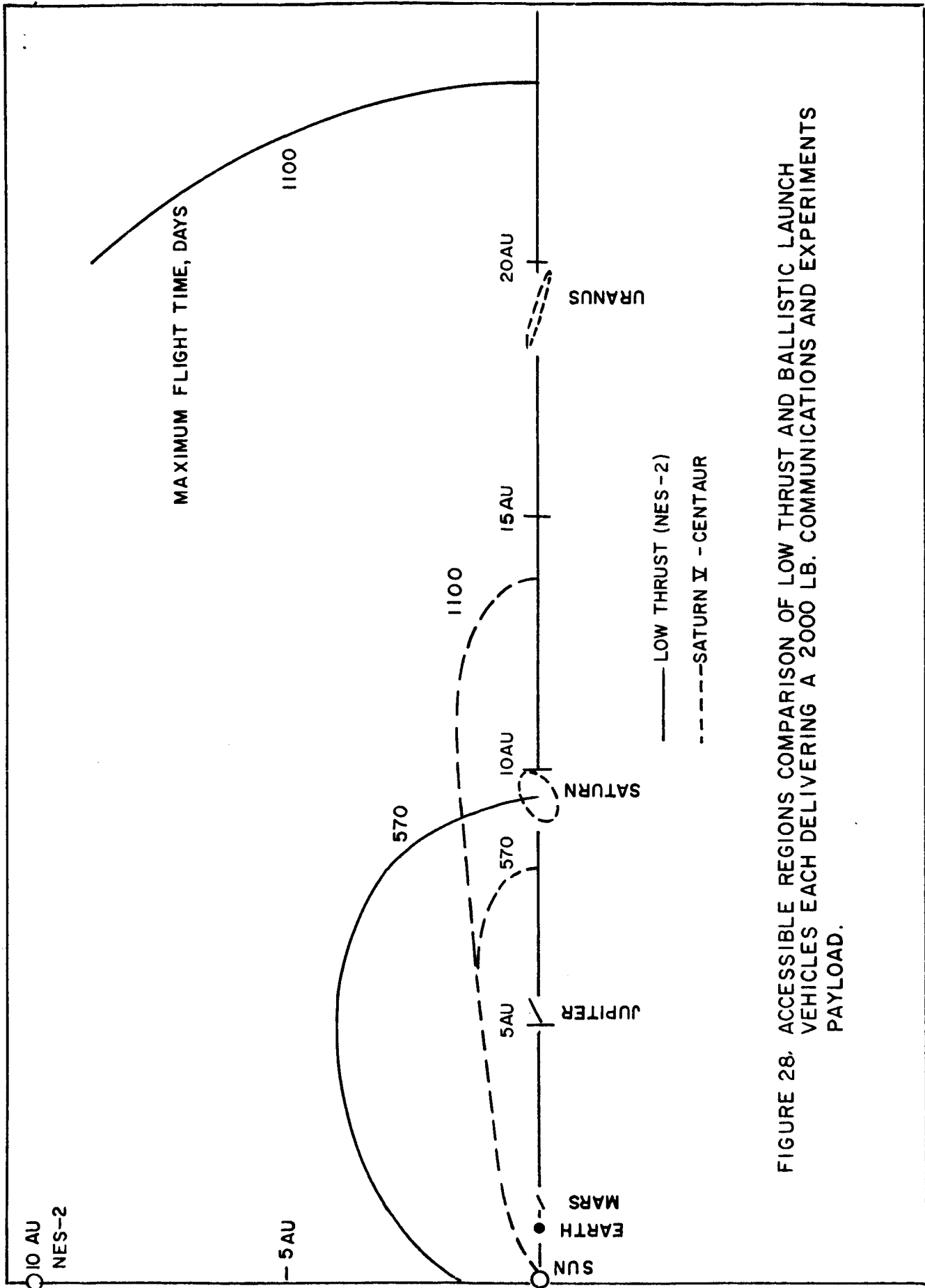


FIGURE 28. ACCESSIBLE REGIONS COMPARISON OF LOW THRUST AND BALLISTIC LAUNCH VEHICLES EACH DELIVERING A 2000 LB. COMMUNICATIONS AND EXPERIMENTS PAYLOAD.

Table 3

FLIGHT TIMES FOR LOW-THRUST MISSIONS
TO THE INNER PLANETS

Mission	Vehicle/C&E Payload Range	
	NES-1 (500-2000 lb)	NES-2 (2000-8000 lb)
Mercury		
Flyby	142-168 days	105-157 days
Capture (parabolic)	270-375	160-340
Orbiter (3 radii)	310-420	175-380
Venus		
Flyby	107-126	78-120
Capture	153-180	120-170
Orbiter	195-237	145-225
Mars		
Flyby	147-172	112-163
Capture	188-220	144-207
Orbiter	210-250	155-235

Table 4

FLIGHT TIMES FOR LOW-THRUST MISSIONS
TO THE OUTER PLANETS

Mission	Vehicle/C&E Payload Range	
	NES-1 (500-2000 lb)	NES-2 (2000-8000 lb)
Jupiter		
Flyby	460-530 days	360-510 days
Capture (parabolic)	720-830	560-790
Orbiter (3 radii)	1390-1740	930-1610
Saturn		
Flyby	720-850	560-800
Capture	1160-1350	900-1290
Orbiter	1620-1980	1150-1840
Uranus		
Flyby	1210-1410	930-1340
Capture	1920-2200	1500-2100
Orbiter	2240-2650	1690-2480
Neptune		
Flyby	1650-1950	1280-1840
Capture	2610-3060	2010-2880
Orbiter	3010-3600	2240-3400
Pluto		
Flyby	1700-2000	1320-1890
Capture	2650-3140	2050-2960
Orbiter	2920-3500	2200-3280

6. CONCLUSIONS

Trajectory energy requirements (in terms of $J = \int_0^{T_f} a^2 dt$) for low-thrust flight throughout the solar system has been presented for (1) the general class of flyby missions to points in and above the ecliptic plane, and (2) flyby, capture and orbiter missions to the planets Mercury through Pluto. Results for the general flyby missions are given in the form of accessible regions contours of J and flight time, while results for the planetary missions are presented as graphs of J versus flight time. The parameter J is analogous to ΔV requirements for ballistic flight in that performance curves of payload versus J may be derived for specific electric spacecraft designs. The summary of J requirements given here should therefore be useful in future mission surveys to estimate the capabilities of electric propulsion systems and their comparison with chemical or nuclear propulsion.

The performance potential of electric propulsion systems is particularly in evidence for those missions having very high energy requirements. On the basis of results described in this report and previous comparisons between ballistic and thrust flight, the most attractive applications of electric propulsion can be identified with solar probes, out-of-the-ecliptic probes, Neptune and Pluto flybys, minimal capture orbiters at Uranus and beyond, and low altitude circular orbiters about all the outer planets. Other mission possibilities include intercept and rendezvous with comets and asteroids.

The principal deterrents to the use of nuclear-electric propulsion systems are the probable high cost of their development, the high powerplant weights currently estimated, and the uncertainty of attaining long operating lifetimes. Their excellent performance potential for accomplishing many missions of future interest is, however, clearly demonstrated. Early solution of the technological problems would therefore open up a new era of space exploration.

Appendix A

NOMENCLATURE

a	Thrust acceleration, m/sec^2
a_0	Initial thrust acceleration, m/sec^2
g_0	Earth surface gravity, 9.806 m/sec^2
I_{SP}	Specific impulse, sec
J	Integral of $a^2 dt$, m^2/sec^3
M	Vehicle mass, kg
M_0	Initial mass, kg
M_{PL}	Net payload mass, kg
M_{PP}	Powerplant mass, kg
P_j	Kinetic jet power, watts
T	Flight time, sec
T_f	Total flight time, sec
α_j	Specific mass of powerplant, kg/watt

Subscripts

C	Refers to planet-capture phase
E	Refers to Earth-escape phase
H	Refers to heliocentric transfer phase

REFERENCES

- Brown, H. and Taylor, J. R. 1966, "Navigator Study of Electric Propulsion for Unmanned Scientific Missions," NASA CR-565.
- Fimple, W. R. and Edelbaum, T. N. 1965, "Applications of SNAP-50 Class Powerplants to Selected Unmanned Electric Propulsion Missions," J. Spacecraft and Rockets No. 5, pp 669-676.
- Friedlander, A. L. 1965, "Low-Thrust Trajectory and Payload Analysis for Solar System Exploration Utilizing the Accessible Regions Method," ASC/IITRI Report No. T-14, Contract No. NASr-65(06).
- Friedlander, A. L., and Narin, F. 1966, "Low-Thrust Trajectory and Payload Analysis for Solar System Exploration," paper presented at Fourth Aerospace Sciences Meeting, AIAA, Los Angeles, June 27-29.
- Lubarsky, B. and Shure, L. 1966, "Application of Power Systems to Specific Missions," presented at Space Power Systems - Advanced Technology Conference, Lewis Research Center, August 23-24.
- Melbourne, W. G. 1961, "Interplanetary Trajectories and Payload Capabilities of Advanced Propulsion Vehicles," JPL TR 32-68.
- Narin, F. 1964, "The Accessible Regions Method of Energy and Flight Time Analysis for One-Way Ballistic Interplanetary Missions," ASC/IITRI Report No. T-6, Contract No. NASr-65(06).
- Richardson, D. E. 1963, "Optimum Thrust Programs for Power-Limited Propulsion Systems Programmed for the IBM 7090 Computer," JPL EPD-179.
- Zola, C. L. 1964, "Trajectory Methods in Mission Analysis for Low-Thrust Vehicles," NASA Lewis TP-20-63.